DRA

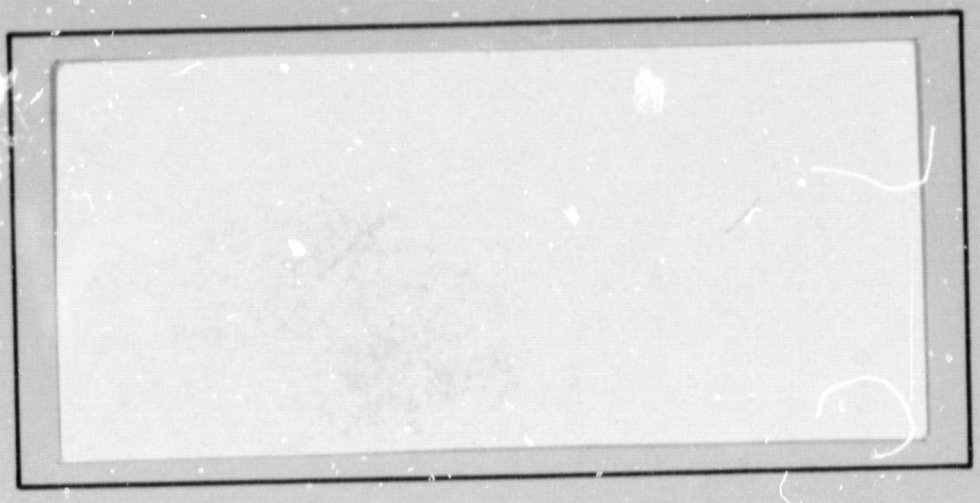

science applications, INC.

(NASA-CR-163902) PHOTOGEOLOGICAL CONSTRAINTS ON LUNAR AND PLANETARY VULCANISM, PART 2 Final Report, 7 Dec. 1978 - Dec. 1979 (Planetary Science Inst.) 120 p HC A06/MF A01 CSCL 03B G3/91

N81-16963

Unclas 16960

PHOTOGEOLOGICAL CONSTRAINTS ON LUNAR & PLANETARY VULCANISM

FINAL REPORT

NASW-3051

PART II

Dec. 5, 1980

Planetary Science Institute
Science Applications, Inc.
283 S. Lake Ave.
Pasadena, CA

ABSTRACT

This is the Final Report on Tasks 3 and 4 of the program "Photogeological Constraints on Lunar and Planetary Volcanism" which was performed between Dec. 7, 1978 and Dec. 7, 1979. The objectives of the program were to develop an understanding of the physical mechanism of thermal erosion by geophysical fluids.

In Task 3A we attempted to develop a conceptual understanding of thermal erosion. We developed a simple one dimensional model of the process for a substrate with temperature dependent viscosity in which erosion was specified to occur when the substrate reached a critical value. This model predicted a square root law dependence of erosion on time whereas common sense considerations indicate a roughly linear relationship. The model was modified to include a convection term yielding the expected linear relationship between erosion and time.

In Task 3B we explored some simple two dimensional models in which the downstream dimension was explicitly included in the model. All the models examined had simple analytical solutions and were primarily developed to improve our understanding of different aspects of the physics of the thermal erosion process. In the first 2D model we calculated the thermal and velocity fields for a steady state flow of a fluid of temperature - independent viscosity with a constant heat

influx at the base of the flow. The calculated velocity has a parabolic dependence on depth. However, the temperature depends linearly on downstream distance with both quartic and quadratic components in depth dependence. We also examined the conditions for turbulent and fully developed flow in the context of this model. It appears that lava erosion flows may be turbulent or laminar but will almost certainly be fully developed.

Our second simple two dimensional model included an examination of the effect of a finite yield stress on flow. Flowing lava behaves as if it has a finite yield stress forming slabs of finite thickness. We showed schematically that thermal erosion by a Bingham fluid results in initial accretion (deposition) of material; net erosion will only occur with a sustained flow. We regard this concept as important to understanding the reasons for lava accretion and erosion in geologic settings.

In a final 2D model we attempted to account in a purely phenomenological way for the effects of turbulence and mechanical erosion in a flow. We adopted criteria for mechanical erosion related to the basal stress and we parameterized the effect of entrained eroded material on fluid properties. A predicted downstream slope profile was generated for steady state erosion.

In Task 4 we extended the earlier work to include laboratory simulation and two dimensional finite element models. In the laboratory simulations with hot wax (Task 4A) we confirmed that when a hot fluid crosses an erodible substrate, accretion occurs initially and erosion will only occur if the flow is sustained. We also showed that the amount of erosion is greatest nearest the source and the crossover point between net erosion and accretion propagates downstream with time. The evolution of the cross section of a thermal erosion channel was also examined. This work was performed by Jose´ Helu´. In Task 4B we developed two dimensional finite element models to simulate lava erision. This work was initially carried out by Wm. James Roberts with the assistance of Jose´ Helu´. However, when Roberts left the Institute in September of 1979, the work was continued under the direction of the Principal Investigator with the assistance and support of Stephen J. Keihm.

Model results were generated for lava flows with three different velocities (10cm/sec, 100cm/sec, and 1000cm/sec) each lasting for 96.7 hours. Plots were generated at intervals of approximately 20 hours for each model and showed the propagation of isotherms relative to the original interface between a lava flow and substrate. Plots of single models showed how the position of the 600°C isotherm varied with time in a given model and contrasted the loci of the 600°C isotherm at the end of each of the three experiments.

In general as the velocity of the flow was increased the isotherms propagated more rapidly into the substrate which equates with more rapid erosion. Propagation is most rapid near the source of fluid. A logical next phase in these modelling efforts is to generate an explicit description for removal of material which could be compared with the experimental results but the best method for doing this is by no means clear.

Data and concepts presented in this report are being included in an article on thermal erosion of martian channels which is in preparation and will be submitted to Icarus.

TABLE OF CONTENTS

TASK 3: THEORETICAL MODELLING STUDY OF LAVA EROSION

The use of several simple theoretical modelling approaches in simulating lava erosion were evaluated under this task. At the outset, when we planned this program, we perceived that a one dimensional model, with properties invariant in the downstream direction, was not suited to modelling a process with inherent variations in the direction of flow. However, such an approach had been taken by previous workers and we decided to try it in order to establish a link with previous work. The one dimensional studies turned out to be limited in scope; we have also examined some highly simplified two dimensional models as a part of this task. The results of these investigations are summarized below.

A. Simple One Dimensional Model

In the treatment of lava erosion given by Carr 1974, the complex intertwined relationships of the thermal and velocity fields in the downstream dimensions are ignored. The lava erosion problem reduces to a simple problem of thermal diffusion. The problem was examined for a channel with an initially rectangular cross-section.

Carr originally treated the lava erosion process in terms of a yield stress. When the substrate is heated to the yield temperature the material of the channel walls immediately participates in the flow. The thermal burden placed on the flow by eroded material was not assessed; neither was the rate at which material could be assimilated and mixed.

Both of these effects are very difficult to model using the yield stress formulation. For this reason, we first looked at a one dimensional erosion model in which substrate changes from solid to liquid over a range of temperatures and not at a single yield point.

1) Simple one dimensional numerical modelling - temperature dependent viscosity - conduction only

This model was originally developed as part of a preposal pilot study. The model is described in detail in Appendix 3.1 and the results illustrated in Fig. 3.1.

The depth of erosion, was (somewhat arbitrarily) defined as the depth at which the substrate velocity falls below some critical value. This curious definition is needed because the semi-infinite character of the boundary conditions permits no net removal or addition of substrate material.

The model probably overestimates the time needed to remove one meter of substrate as it incorporates no mechanism for bringing fresh hot lava into contact with the substrate. The amount of erosion is proportional to the square root of time over a broad range of times and lava temperatures. This behavior is to be expected from the constraints of the model as described above but is not expected for real world lava erosion which is likely to more closely approach a linear law. Downstream variation in erosion and accretion is not part of the model. Finally, we did not include the temperature dependence of rock conductivity (Appendix 3.2).

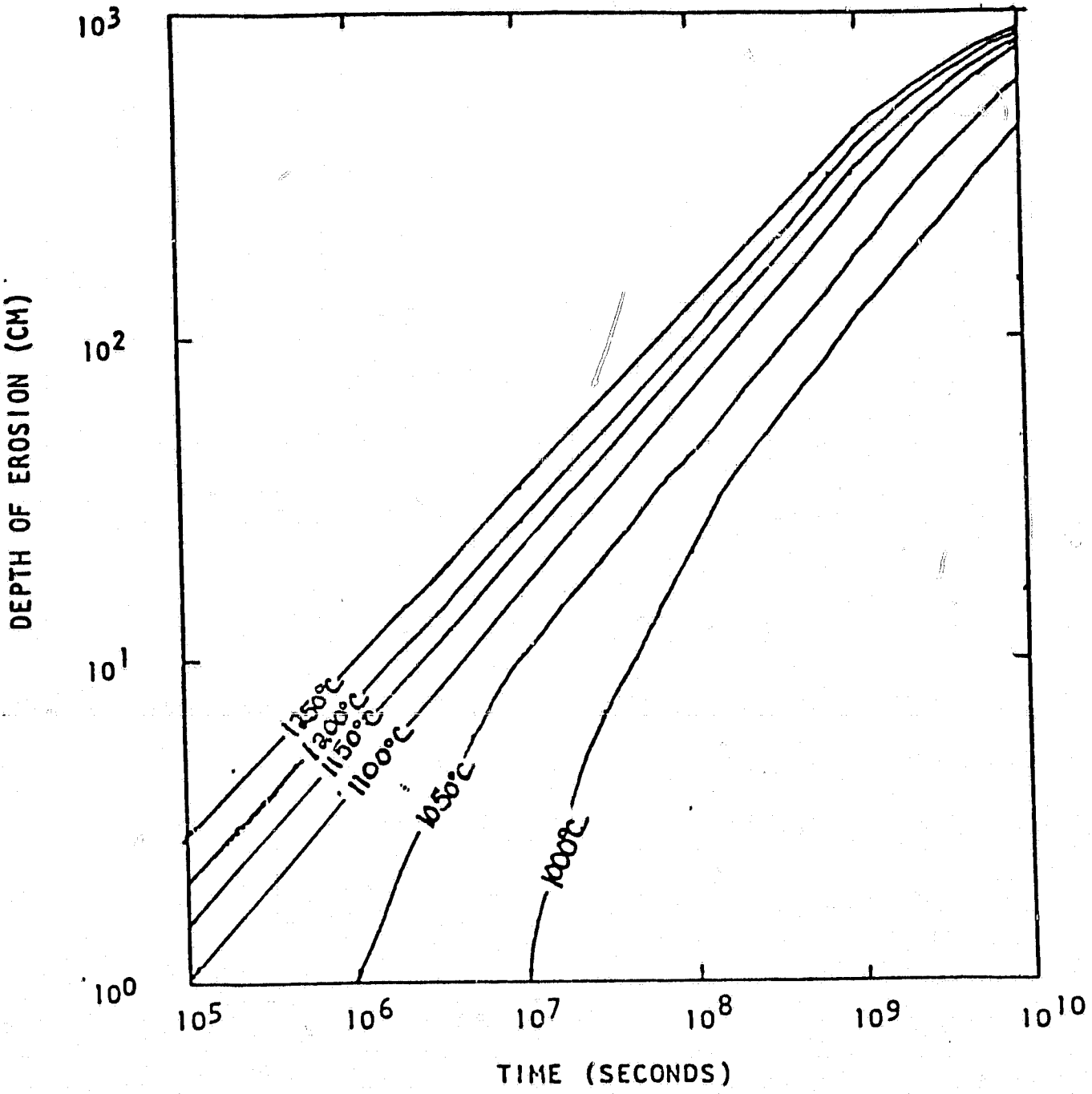

Fig. 3.1 Results of simple temperature dependent viscosity model of lava erosion.

2) Simple one-dimensional numerical modelling - temperature-dependent viscosity - conduction and convection

Some of the deficiencies of the "one-dimensional-conduction-only" model can be rectified by including a convection term to permit faster transfer of heat than allowed by conduction alone. We have assumed that material at all levels above the level with temp. T_{thr}, and therefore, viscosity ν_c, are mixed in a time interval t_m. Our specific implementation of this model also allows the addition of hot lava from upstream.

A grid of 14 nodes (depths) at which temperature is defined is set up. Another similar grid is set up "upstream" of it and filled with hot fluid. At each time step, first the convection and conduction terms are evaluated and new temperatures are defined, all using only the main grid. Next, hot fluid is introduced from the upstream "reservoir" grid, as a function of the temperature in each main grid element. This simulates in a crude fashion the viscosity-dependent addition of hot lava from upstream. If a node is below $T=T_{thr}$, no addition of hot lava takes place. If a node is above $T=T_{hiv}$, then the node is completely replaced by hot lava. For $T_{thr}<T<T_{hiv}$, the amount of replacement of partially melted material with hot lava depends linearly on T (Fig. 3-2). New main grid temperatures are then defined taking this into account, and the cycle repeats.

In Fig. 3.3 and 3.4 we show some results calculated with this model. Because the parameters of hot wax were used in this calculation the results cannot be directly compared with results shown in Fig. 3.1. However, the total erosion depends linearly on time

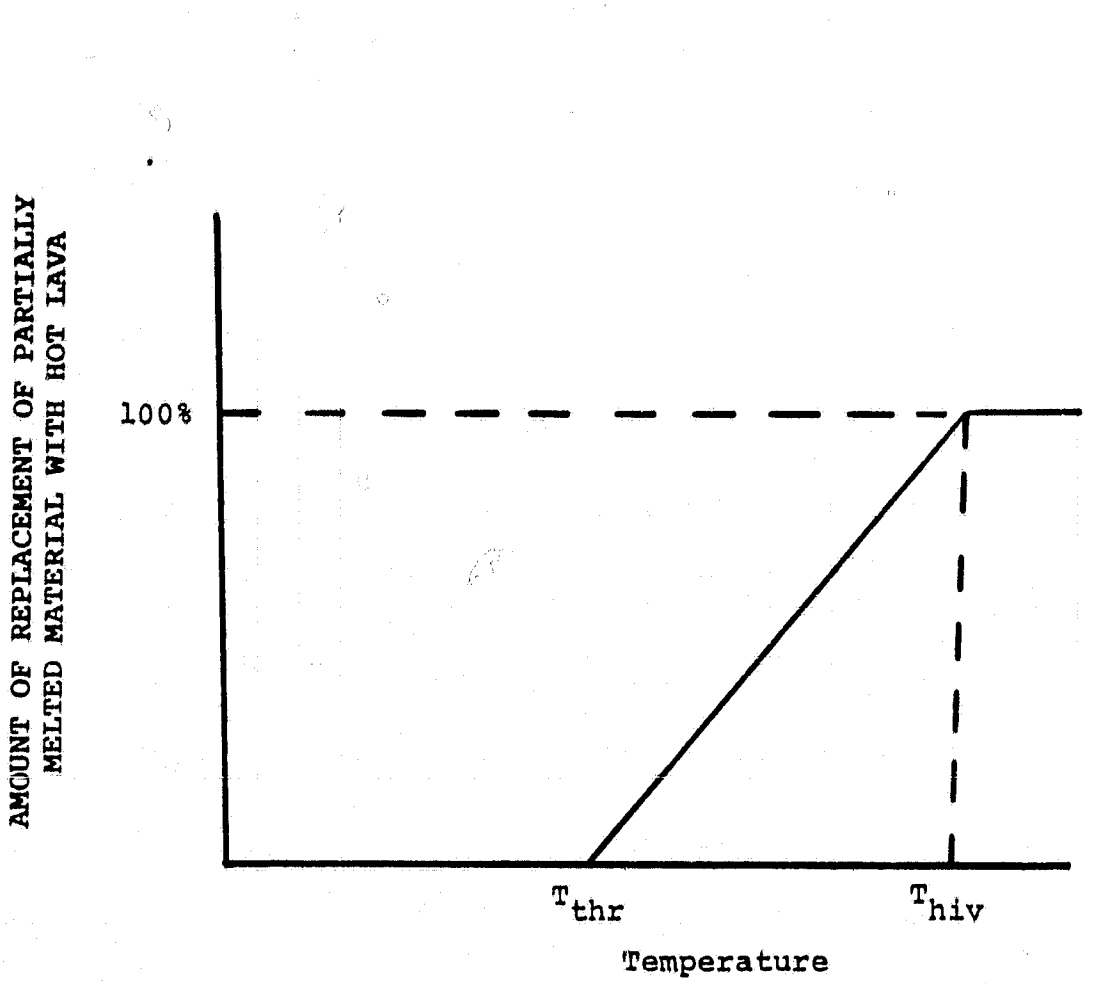

Fig. 3.2 The percent replacement by hot lava as a function of lava temperature for the one dimensional model with conduction and convection.

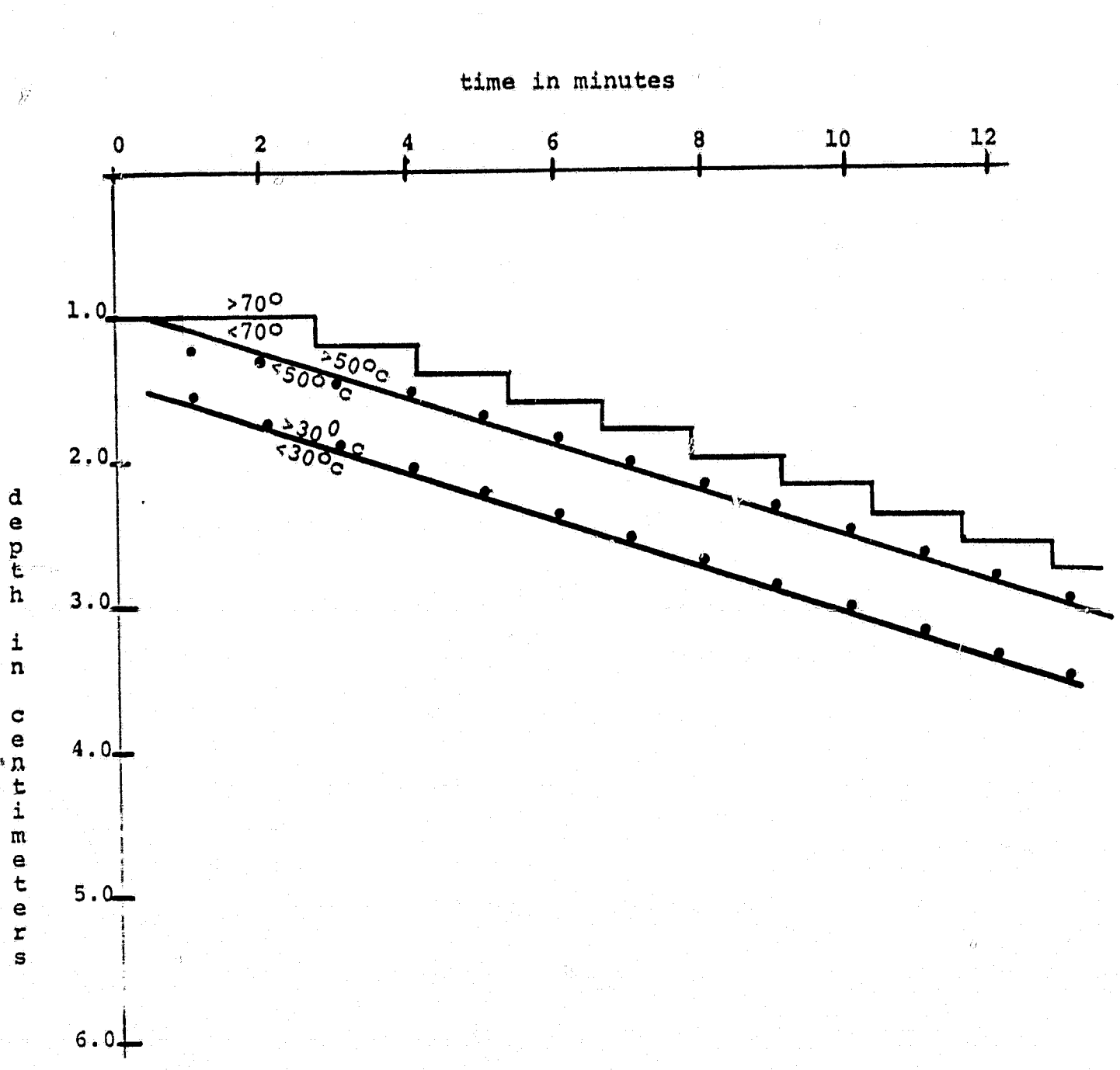

Fig. 3.3 Erosion as a Function of Time for One Dimensional Model with Conduction. The Result is Linear as Expected.

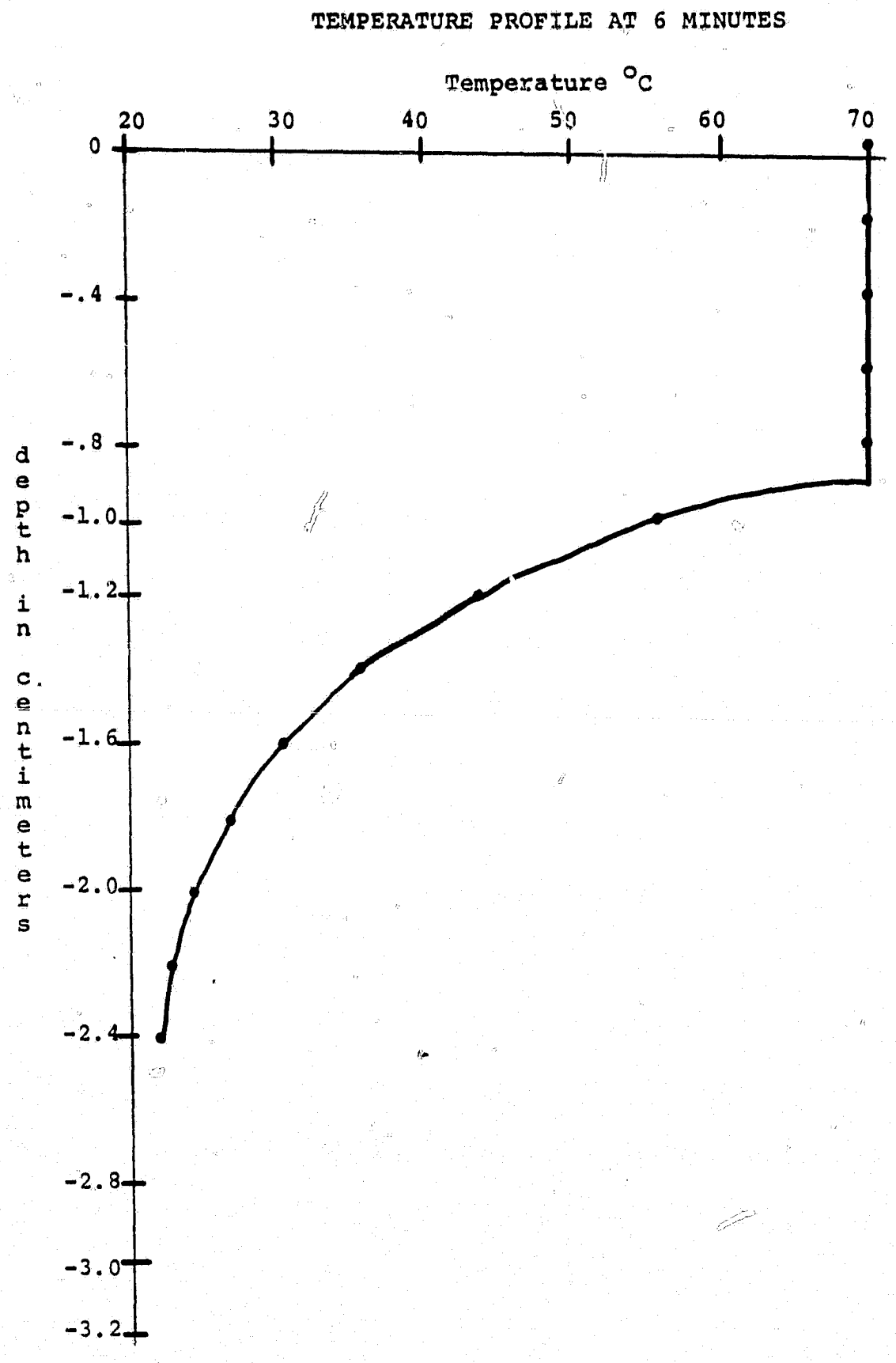

Fig. 3.4 Temperature Profile as a Function of Time for Simple One Dimensional Model with Conduction and Convection.

as expected in contrast with the simple conduction model (Section 3A1). The typical temperature profile using the hot wax parameters (Fig. 3.4) shows a sharp break in the temperature gradient at the fluid base.

The methods used above to simulate non-conductive heat transport are obviously crude. The mixing model could be improved upon using numerical or parameterized theories of convection but the simulation of advection of heat from upstream is obviously not capable of rigorous treatment in purely one dimensional terms. The two dimensional treatment is needed to accomplish this.

B. Simple Two Dimensional Models

1) Simple two dimensional models - laminar flow

Simple models with analytic solutions for the thermal and velocity fields are sometimes useful for understanding the physics of a flow process. Such a model has these attributes: the flow is assumed to be in a steady state and basal heat flow is uniform at all places along the flow. We also ignore the heat generated by fluid friction and assume that fluid viscosity is independent of temperature. The geometry of this model is shown in Fig. 3.5(a).

Velocity Field

The Navier Stokes equations describing the flow of mass and momentum in an incompressible fluid with constant viscosity are given in Bayley Owen and Turner (Eq. 5.15).

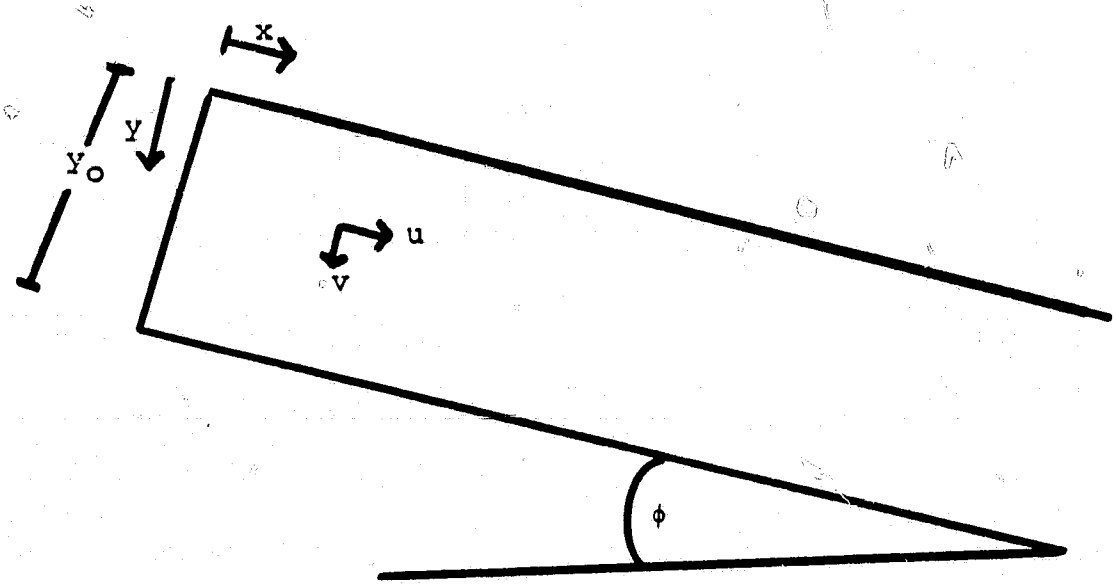

Fig. 3.5a Geometry of simple 2 two dimensional laminar flow model of fluid viscosity indep of temperature.

$$\rho\left(u\frac{\partial u}{\partial x} + v\frac{\partial u}{\partial y}\right) = F_x - \frac{\partial p}{\partial x} + \mu\left(\frac{\partial^2 u}{\partial x^2} + \frac{\partial^2 u}{\partial y^2}\right) \qquad 3.B.1$$

$$\rho\left(u\frac{\partial v}{\partial x} + v\frac{\partial v}{\partial y}\right) = F_y - \frac{\partial p}{\partial x} + \mu\left(\frac{\partial^2 v}{\partial x^2} + \frac{\partial^2 v}{\partial y^2}\right) \qquad 3.B.2$$

where ρ = density

x, y = positional coordinates

u, v = velocities

F_x = component of body force along

p = pressure

μ = dynamic viscosity

Under conditions of steady flow along a plane:

$v = 0$ everywhere 3.B.3

$u = u(y)$ and is therefore independent of x 3.B.4

$\frac{\partial u}{\partial x} = 0$ everywhere 3.B.5

$\frac{\partial u}{\partial y}$ = is independent of x 3.B.6

$\frac{\partial^2 u}{\partial x^2} = 0$ 3.B.7

$\frac{\partial^2 u}{\partial y^2}$ = is independent of x 3.B.8

$F_x = \rho g \sin\phi$; $F_y = \rho g \cos\phi$ 3.B.9

Substituting these conditions in (3.B.1) and (3.B,2) we obtain

$$F_x = \mu\frac{\partial^2 u}{\partial x^2} = \rho g \sin\phi \qquad 3.B.10$$

$$F_y = \frac{\partial p}{\partial y} = \rho g \cos\phi \qquad 3.B.11$$

Integrating equation (3.B.10) once

$$\frac{\partial u}{\partial y} = \frac{\rho g \sin\phi}{\mu} \cdot y + C_1 \qquad 3.B.12$$

At $y = 0$, $\frac{\partial u}{\partial y} = 0$, therefore $C_1 = 0$

Integrating again

$$u = \frac{\rho g \sin\phi}{2\mu} \cdot (y_0^2 - y^2) \qquad 3.B.14$$

The mean velocity

$$\bar{u} = \frac{\int_0^{y_0} u \, dy}{\int_0^{y} dy}$$

$$= \frac{\rho g \sin\phi}{2\mu y_0^2} \int_0^{y_0} 1 - \frac{y^2}{y_0^2}$$

$$= \frac{\rho g \sin\phi \, y_0^2}{3} = \frac{2}{3} U \text{ max} \qquad 3.B.15$$

Thermal Field

For an incompressible fluid the energy equation for the flow can be expressed using equation 5.42 (b) of Bayley Owen and Turner as

$$\rho c_p \left(u \frac{\partial T}{\partial x} + v \frac{\partial T}{\partial y}\right) = k\left(\frac{\partial^2 T}{\partial x^2} + \frac{\partial^2 T}{\partial y^2}\right) + u\phi \qquad 3.B.16$$

The energy equation shows that convective heat transfer due to fluid motion is balanced by work due to volumetric changes, the heat conducted through the fluid and viscous dissipation. It doesn't contain potential energy terms as these are implicit within the other energy terms.

Under the conditions of steady flow down a plain then $v = 0$ everywhere. Other conditions are that the basal heat flow (q_s) is constant and ϕ is negligible. We adopt a further contraint on a solution that $\frac{\partial^2 T}{\partial x^2} = 0$ throughout the flow which is the condition for a steady state fully-developed flow. Equation (3.B.16) reduces to:

$$u \frac{\partial T}{\partial x} = \alpha \frac{\partial^2 T}{\partial y^2} \qquad 3.B.17$$

where $\alpha = \frac{k}{\rho C_p}$ = thermal diffusivity with boudary conditions:

$$-k\left(\frac{\partial T}{\partial y}\right) y = y_0 = q_s \qquad 3.B.18$$

$$\left(\frac{\partial T}{\partial y}\right) y = 0 = 0 \qquad 3.B.19$$

From the velocity solution equation (3.B.14)

$$u = \frac{\rho g \sin\phi}{2\mu} (y_0^2 - y^2) = C_1 (y_0^2 - y^2) \qquad 3.B.14A$$

We will look for a solution satisfying (3.B.14, 3.B.17, 3.B.18), and 3.B.19

$$T = T_1 G(y) + T_2 x \qquad 3.B.20$$

where $G(y = y_0) = 0$, such that the surface temperature of the lava equals the temperature of the plane on which it flows.

Evaluating derivatives of (3.B.20)

$$\frac{\partial T}{\partial x} = T_2; \quad \frac{\partial T}{\partial y} = T_1 G^1(y); \quad \frac{\partial^2 T}{\partial y^2} = T_1 F^{11}(y) \qquad 3.B.21$$

Substituting in equation (3.B.17)

$$uT_2 = \alpha T_1 G^{11}(y)$$

$$G^{11}(y) = \frac{T_2}{\alpha T_1} \cdot C_1 (y_0^2 - y^2) \qquad 3.B.22$$

Integrating equation (3.B.22) once:

$$G^1(y) = \frac{T_2}{\alpha T_1} \cdot C_1 \left(y_0^2 y - y^3/_3\right) + D_1 \qquad 3.B.23$$

At $y = 0$ $\left(\frac{\partial T}{\partial y}\right) = 0$ and, substituting in (16) $D_1 = 0$

At $y = y_0$ $\left(\frac{\partial T}{\partial y}\right) = -qs/_R$ and substituting in (3.B.23)

$$T_2 = \frac{\alpha 3\ q_s}{2R\ C_1\ y_0^3} \qquad 3.B.24$$

Now integrating (3.B.23) with D_1 set to zero.

$$G(y) = \frac{T_2}{\alpha T} \cdot C_1 \left(y_0^2\ \frac{y^2}{2} - \frac{y^4}{12} + D_2\right) \qquad 3.B.25$$

and substituting for T_2

$$G(y) = \frac{3\alpha g_s}{2k\ y_0^3\ \alpha T_1} \left(y_0^2\ y^2/_2 - \frac{y^4}{12} + D_2\right) \qquad 3.B.26$$

at $y = 0$, $G(y) = 0$ and $D_2 = \frac{-5y \cdot 4}{12}$ and substituting in equation (13) for T_1, T_2 and $G(y)$

$$T = \frac{q_s}{8k\ y_0^3} \left[5 y_0^4 - 6 y_0^2 y^2 + y^4 - \frac{12xx\mu}{\rho_g \sin\phi}\right] \qquad 3.B.27$$

The computer program in Appendix 3.3 calculates the velocity-temperature field using the relationships developed above.

The essential features of the model as illustrated by the model results in Fig. 3.5(b) and (c) are that basal temperature decreases linearly with distance in the direction of flow (this assumes that heat is being conducted downwards from the fluid). The variation of temperature with depth involves quadratic and quartic terms. The depth profile of temperature has the same

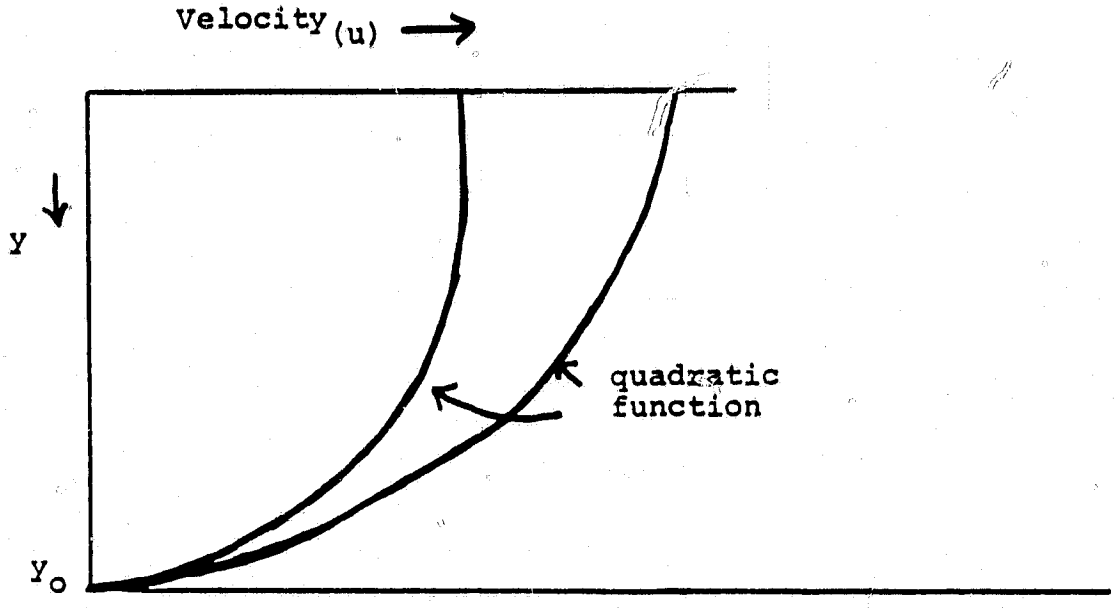

Fig. 3.5(b) Dependence of velocity on depth

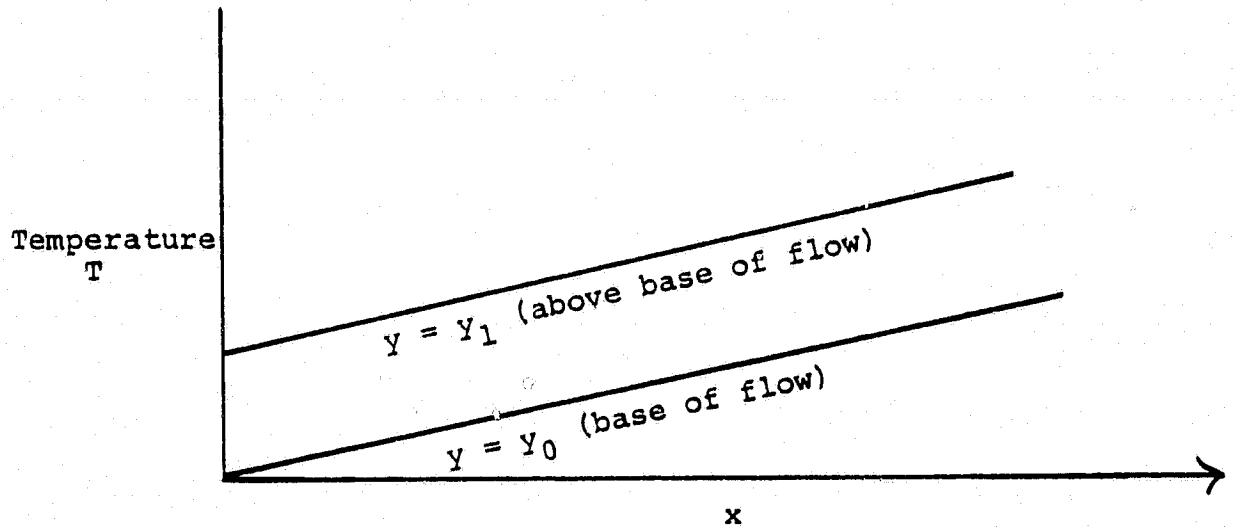

Fig. 3.5(c) Dependence of temperature on downstream distance

shape at all points along the channel because T in equation is separable in x and y. The model has no direct application to the lava erosion problem although it does indicate what the temperature distribution in a fluid coming into contact with a conducting surface must be in order to bring convective and conductive heat transport into balance.

2) Simple two dimensional models - conditions for turbulent and fully developed flow

In the analysis of the simple laminar flow model given in the last section we did not address whether the laminar flow model is appropriate to flow conditions experienced during thermal erosion and we did not consider the boundary layer relationships that can be expected when a flow first comes into contact with a substrate.

Laminar vs. Turbulent Flow

According to Carr (1973) the mean flow velocity in a channel for laminar flow can be related to the hydraulic slope, channel dimensions, and physical parameters of the fluid as follows:

$$v = \frac{\rho g r_h^2 \sin\phi}{3\eta} \qquad 3.B.28$$

where g = acceleration of gravity

$\sin\phi$ = hydraulic slope

r_h = hyraulic radius = CSA ÷ wetted perimeter

η = viscosity

This equation is applicable when R (Reynolds number) < 1000: for common basaltic layer viscosities of 10^3 to 10^4 poise the flow doesn't get turbulent in channels of hydraulic radii 10m or so until the velocity reaches about 3m/sec (Appendix 3.3). Solving for $\sin\phi$ in equation 3.B.28.

$$\sin\phi = \frac{3V\eta}{\rho g r_h^2}$$

$$= 3 \times 3 \times 10^2 \times 10^3$$

$$3 \times 371 \times 10^6$$

$$= \frac{1}{1.000} = 0.06^\circ$$

So the steepness of slope required for the lava to flow is only about $.06^\circ$. (Carr gets 100 times this. We have not checked his arithmetic to see if there is an error.) In his chart for $\eta = 10^3$ and $r_h = 10^3$, Carr shows the transition occurring at a slope of about 0.5° and at a velocity of about 3×10^2 (~3m/sec). However, just at $\eta = 10^4$ the turbulent transition has moved up to a higher velocity and the turbulent transition doesn't occur until one gets to a slope of 3.44°. Thus in the range of from 10^3 to 10^4 and for hydraulic radii of 10 meters or so the onset of turbulence is very sensitive to the viscosity.

Entry Length - Velocity and Thermal Boundary Layers

Where a fluid first encounters a surface with a no slip condition a boundary layer will begin to form. The entry length (l_e) is the distance from this point to that point

downstream where the boundary layer thickness has grown to encompass the entire depth of the fluid.

Entry lengths have been determined by fluid dynamicists for a number of problems with simple geometry. For example for a flow into a tube the hydrodynamic entry length (l_e) is given by:

$$l_{e/d} = 0.0575\ Rd \qquad 3.B29$$

d is pipe diameter and Rd is Reynolds number based on that diameter.

$$Rd = \frac{\rho \bar{v} d}{\mu} \qquad 3.B.30$$

For laminar flow, Rd is <<1000 and flow becomes fully developed fairly close to the mouth of the tube. Analysis have also been conducted of flows over isothermal plates (Bayley, et al, 1972) which are more relevant to the geometry of the lava erosion problem.

The entry lengths for thermal and velocity boundary layers are not identical. The Prandtl number (P) governs the relative thickness of the velocity and thermal boundary layers.

$$\delta v = P^{\frac{1}{2}} \delta T \qquad 3.B.31$$

The Prandtl number is solely a function of fluid properties and can be regarded as the ratio of kinematic viscosity v^∞ to the thermal diffusivity α^∞ where $v^\infty = k/(\rho_\infty C\rho)$

$$P = \frac{v^\infty}{\alpha^\infty} \qquad 3.B.32$$

For lava (see Appendix 3.3) the kinematic viscosity is just a factor of 3 smaller than the viscosity $\nu \approx 300$ Stokes. The thermal diffusivity of an Apollo basalt lies between 3 and 7×10^{-3} cm^2/sec* in the range 100^oK to 400^oK and as shown in Appendix 3.4 really does not increase much due to radiation even at high temperatures. Consequently a good value for the Prandtl number is:

$$\underline{P} = \frac{10^3}{5 \times 10^{-3}} = \underline{2 \times 10^5}$$

and the ratio of the thickness of the boundary layer is $\delta v/\delta_T = (2 \times 10^5)^{\frac{1}{2}} \approx 450$.

In a situation where the hydrodynamic entry length is of the order of 10 times the fluid depth, then the flow does not become fully developed thermally until it reaches a distance of some 5000 times the fluid depth from the source. For a fluid depth of 10m, this distance is 50km; for 100m depth it is 500km. Consequently the flows carving long channels will be fully developed for most of their length unless they were formed by very deep flows.

3) Simple two dimensional models - effects of a finite yield stress (Bingham properties)

Recent research into the behavior of accreting lava flows conducted by Hulme (1974, 1976) suggests that the flow of lava cannot simply be modelled by a viscosity. Here we review

---

*Carr quotes a value 5 to 10 times higher based on the work of Murase and McBirney.

Hulme's work and its significance to the investigation of lava erosion.

In an attempt to better account for lava flow dimensions, Hulme (1974, 1976) modelled lavas as Bingham fluids - fluids which do not flow until the stress exceeds a yield stress and then flow at a rate determined by the excess of the actual stress over the yield stress. According to this model a flow will rapidly spread until it thins to a critical thickness (T_B) at which the stress at the base of the flow equals the yield stress. Hulme showed that lava effusion rates are normally too high to permit significant cooling of the interior of the lava body before the flow comes to rest. Tensional forces in the more rapidly cooling skin, even without considering its highly fractured character are not sufficient to restrain the flow. Consequently, a finite yield stress in the lava seems to be necessary in order to explain the finite thickness of flows. Even in a very thick Bingham type flow, however there will be heating and possibly yielding of the substrate rock at the base of the flow.

If flowing lava has Bingham properties, then many of the relationships discussed in the last three sections require modification. In addition, it is necessary to take into account an effect which is not present in the purely viscous theory. With a Bingham fluid the thickness of material eroded from the substrate must exceed the critical thickness for

Bingham flow (T_B) before any net erosion can occur. This effect is illustrated schematically in Fig. 3.6. Depending on the flow regime, the amount of erosion taking place at th base of the flow will be best represented by either the purely conductive relationships presented in Section A1 or the advective relationships presented in Section A2.

4) Simple two dimensional models - phenomenological model of thermo-mechanical erosion

A plastic material is a Bingham material with a finite yield stress but zero viscosity. Consider a flow on a surface of varying slopes. A plastic material comes to equilibrium on the slope at a rate only determined by inertial forces. A Bingham fluid with the same critical shear stress as the plastic fluid, but with a finite viscosity, will take longer to reach equilibrium than the purely plastic fluid. However, it will ultimately reach an identical equilibrium distribution of flow thickness as the plastic fluid. To evaluate the amount of thermal erosion by a Bingham fluid we must be concerned with the finite thickness of the flow after flow has ceased (Fig. 3.6) as well as the amount of material transported from the substrate. The plastic model can help us to understand the effects of yield stress on the slope profile created by an erosive fluid.

In addition to the contributions to lava erosion by convective and conductive heat transport, we consider the additional

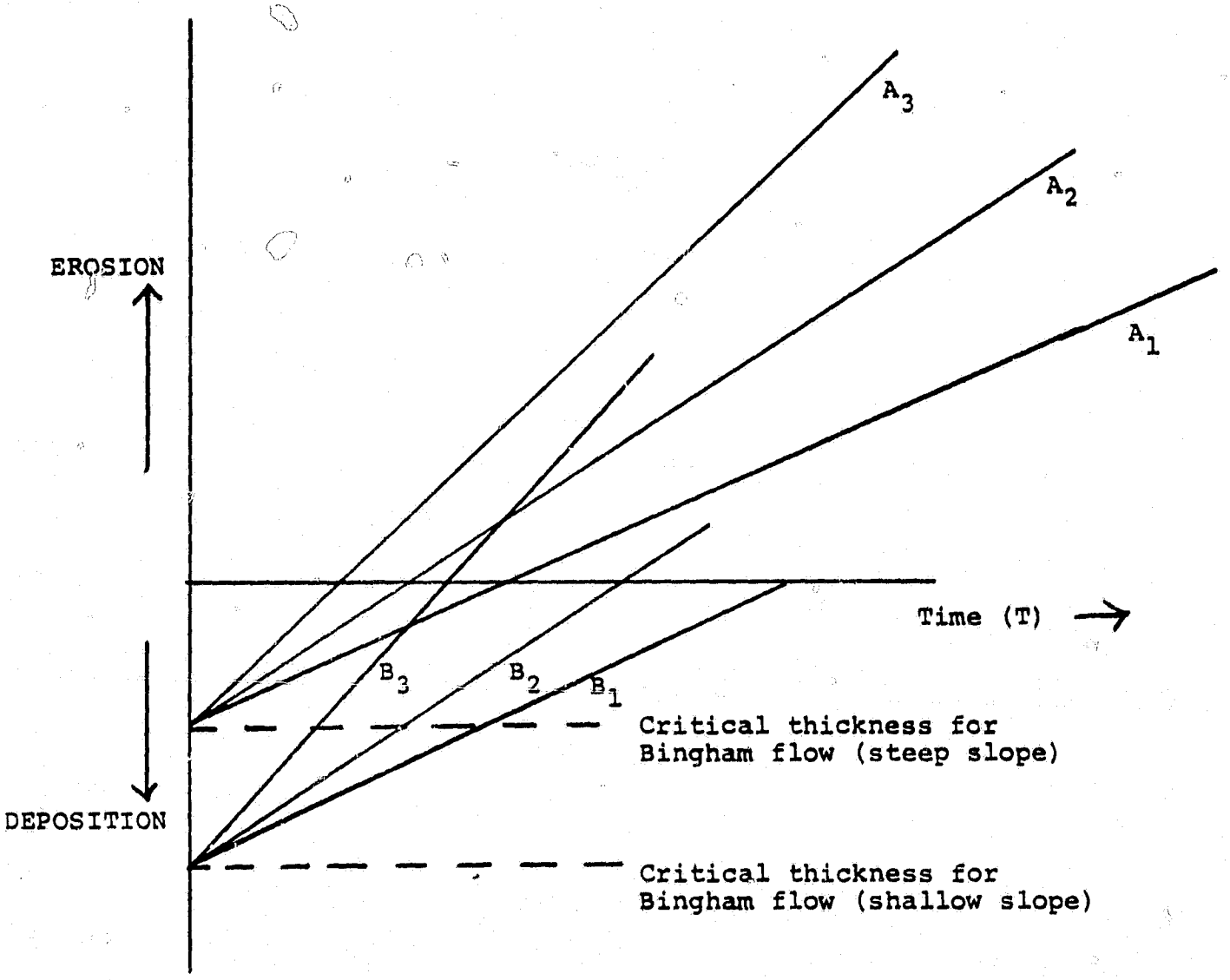

Fig. 3.6 Thermal erosion by a Bingham fluid. Schematic relationships between amount of erosion and time for two values of the critical thickness for Bingham flow. Thermal diffusivity increases resulted in a progressive increase in slope of these cruves and net erosion occurring earlier in time.

mechanical effects that occur when turbulence is present. In such situations blocks of material can be torn away and incorporated in the flow.

A simple phenomenological approach which is applicable when turbulence becomes important and which includes the effects of both mechanical and thermal erosion is examined below. It depends on two assumptions: 1) that there exist simple functional relationships between erosion rate and flow parameters. 2) that solution and mixing of eroded material takes place on a time scale that is small compared to the time taken for material to travel the entire length of the flow. Due to rapid homogenization the temperature of the flow can be taken to be uniform with depth and dependent only on downstream location; 3) that viscous forces (forces proportional to velocity shear) and inertial forces are negligible within the flow. Flow is assumed to be perfectly plastic and controlled by a critical shear stress τ_y. Perfect plasticity is a special case of Bingham plasticity where the plastic viscosity (μ_p) is zero.

First of all we will establish a relationship between the rate at which a flowing lava erodes material and the dynamical parameters of the flow. A very simple model was adopted because our interest is not so much to demonstrate what will actually occur in a given flow, but rather what is energetically possible for a wide range of properties of the lava-substrate interaction.

Let us assume a plastic fluid is doing the eroding and that it is a plana flow (Fig. 3.7) which has a thickness h at any point defined as follows:

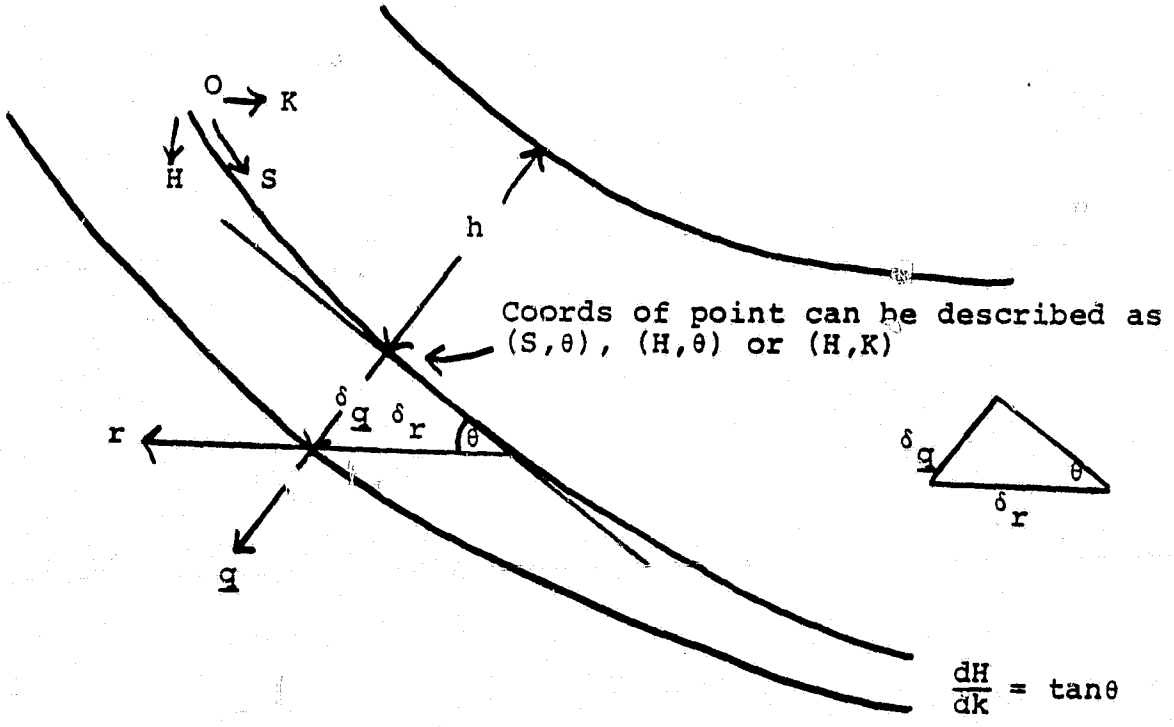

Fig. 3.7 Geometry for a simple model for mechanical lava erosion

$$\tau_p = \rho g \sin\theta \, h \qquad 3.B.33$$

where τ_p = critical basal shear stress for the plastic fluid

ρ = density of fluid

g = acceleration of gravity

θ = slope angle

h = fluid thickness

Let us also assume that the rate of erosion can be expressed just in terms of the basal shear stress ($\tau_B = \tau_p$) and the velocity of the fluid

$$\frac{dq}{dt} = C_e \tau_B^{\,n} \cdot v^m = C_e \tau_p^{\,n} \cdot v^m \qquad 3.B.34$$

where $\frac{dq}{dt}$ = the rate of downcutting of the slope (see Fig. 1)

C_e = constant

v = velocity

m,n = constants

Downcutting may be caused either by thermal or mechanical erosion.

Starting with relationships (3.B.33) and (3.B.34), one approach to the lava erosional problem is to take an initial slope profile and examine how it evolves with time. Another approach is to solve for the slope profile which recedes but otherwise remains invariant with time. We will determine that such a profile does exist and perform the numerical integration

needed to define its form. However, we do not demonstrate that this slope profile is a stable profile and the asymptotic consequence of the erosion of any arbitrary profile.

For uniform slope recession, the rate of downcutting $\frac{dq}{dt}$ can be expressed in terms of this uniform rate of slope recession ($\dot{r}_c$)

$$\frac{dq}{dt} = \dot{r}_c \sin\theta \qquad 3.B.35$$

The fractional mass gain δf by an element of fluid thickness h and width δs in the downstream dimension can be expressed as

$$\delta f = \left(\frac{dq}{dt}\right)_s \delta t = \left(\frac{dq}{dt}\right)_s \cdot \frac{1}{v(s)h(s)} \delta s \qquad 3.B.36$$

For a steady flow the mass flux will increase with s and provided $f << 1$ the mass flux (M(s)) can be expressed as:

$$\begin{aligned} M(s) &= \rho h(s) v(s) \\ &= \rho h(o) v(o) + \int_o^s \left(\frac{dq}{dt}\right)_s \, ds \end{aligned} \qquad 3.B.37$$

For a steady flow the plastic shear stress (τ_p) will also increase downstream due to addition of eroded debris to the flow. Let us assume that a functional relationship between τ_p and f exists of the form

$$\tau_p = G(f) \qquad 3.B.38$$

By integrating equation (3.B.36) τ_p can be expressed in terms of s.

We shall now look at a set of flow conditions of particular interest when a small fractional increase in flow mass f produces a much larger fractional increase in the plastic shear Stress τ_p. In this circumstance we can neglect the increase

in mass flux with s and therefore from equations 3.B.37

$$M(s) = \rho h(s) v(s) = \text{constant} = M_c \qquad 3.B.39$$

Substituting quantities from equations 3.B.35 and 3.B.39 in Equation 3.B.36 and integration:

$$f = \int_o^s \left(\frac{dq}{dt}\right) \frac{1}{v(s)h(s)}\, ds = \int_o^s r_c \sin\theta \cdot \rho/M_c \, ds$$

$$= r_c \rho/M_c \int_o^s \sin\theta \, ds$$

Referring to Fig. 1 we can make a change of variables from θ to H where $\sin\theta = \frac{dH}{ds}$ so that

$$f = r_c \rho/M_c \int_o^s \frac{dH}{ds}\, ds = r_c \rho/M_c \, H(s) \qquad 3.B.40$$

This simple result can be summarized as follows. Under the constant profile constraint for the steady flow condition the mass fraction of eroded material picked up by the flow can be simply expressed as a linear function of the elevation change.

We are now in a position to solve for the shape of the invariant slope profile.

$$\tau_p = \rho g h \sin\theta \qquad 3.B.33$$

$$\frac{dq}{dt} = C_e \tau_p^{\,n} v^m \qquad 3.B.34$$

$$\frac{dq}{dr} = r_c \sin\theta \qquad 3.B.35$$

$$\tau p = G(f) \qquad 3.B.38$$

$$M_c = \rho h v \qquad 3.B.39$$

and

$$f = \dot{r}_c \cdot \rho/M \cdot H \qquad 3.B.40$$

We are looking for a relationship between H and sinθ and so we should attempt to eliminate the variables $\frac{dq}{dt}$, τ_B, h, f, and v using these equations.

A. Eliminate $\frac{dq}{dt}$ between equations 3.B.34 and 3.B.35

$$\dot{r}_c \sin\theta = C_e \tau_p^n v^m \qquad 3.B.41$$

B. Substitute for v in Eq. 3.B.41

$$\dot{r}_c \sin\theta = C_e \tau_p^n \left(\frac{M_c}{\rho h}\right)^m \qquad 3.B.42$$

C. Substitute for τ_B in Eq. 3.B.42

$$r_c \sin\theta = C_e (\rho g h \sin\theta)^n \left(\frac{M}{\rho h}\right)^m \qquad 3.B.43$$

D. Eliminate τ_p from 3.B.33 and 3.B.38

$$\rho g h \sin\theta = G(f) \qquad 3.B.44$$

E. Substitute h from 3.B.44 in 3.B.33

$$r_c \sin\theta = C_e (\rho g \sin\theta)^n \left(\frac{M}{\rho}\right)^m \left(\frac{G(f)}{\rho g \sin\theta}\right)^{n-m} \qquad 3.B.45$$

Rearranging:

$$r_c \sin\theta = C_e \left(\frac{\rho g \sin\theta M}{\rho}\right)^m \cdot (G(f))^{n-m}$$

$$r_c \sin\theta = C_e (gM)^m \cdot (G(f))^{n-m} \cdot \sin^{m-1}\theta$$

$$\sin^{m-1}\theta = \frac{r_c}{C_e (gM)^m} \cdot (G(f)^{m-n}$$

Finally:

$$\sin\theta = \left\{\frac{r_c}{C_e (gM)^m} \cdot \left[(G(r_c \cdot \rho/M_c \cdot H)\right]^{m-n}\right\}^{\frac{1}{m-1}}$$

$$= F(H) \qquad 3.B.46$$

In the H, K coordinate system we can now express dH/dK in terms of H and Θ.

$$\frac{dH}{dK} = \tan\Theta = \frac{\sin\Theta}{(1-\sin^2\Theta)^{\frac{1}{2}}} = \frac{F(H)}{(1-F^2(H))^{\frac{1}{2}}}$$

Thus $$K = \int_0^K dK = \int_0^H \frac{(1-F^2(H))^{\frac{1}{2}}}{F(H)}\, dH \qquad 3.B.47$$

The integral in Eq. 3.B. can be evaluated once we specify G(f) explicitly. One form that approximates the properties of lava is:

$$G(f) = \tau_p\, e^{f/fo} \qquad 3.B.48$$

Substituting in (3.B.46)

$$F(H) = \left\{ \frac{\dot{r}_c}{C_e (gMc)^m} \cdot \tau fo^{m-n} \cdot e^{\frac{m-n}{fo}(r_c\, \rho/M \cdot H)} \right\}^{\frac{1}{m-1}} \qquad 3.B.49$$

$$= (P_o\, e^{H/Ho})^{1/m-1}$$

where $$P_o = \frac{\dot{r}_c}{C_e (gM)^m} \cdot \tau_{po}^{m-n} \qquad 3.B.50$$

and $$\frac{1}{Ho} = \frac{m-n}{fo} (\dot{r}_c \cdot \rho/M) \qquad 3.B.51$$

K can then be calculated using Eq. 3.B.47.

A program for integrating equation 3.B.47 (Appendix 3.5) allows the functional relationship between H and K to be determined for selected values of B, Q, and m. Some results appear in Figs. 3.8 and 3.9. A more advanced program is in preparation which allows the calculation to be made in terms of the more basic parameters and also calculates the other parameters of interest τ_p, f, v, and h as these vary along the flow.

The analytical solution described above is only practical with the condition that slope remains invariant. We have applied numerical techniques to modelling of the evolution of slope profiles of arbitrary initial slope. These calculations were performed as part of Task 4 and are described in our report on that task which appears in this document.

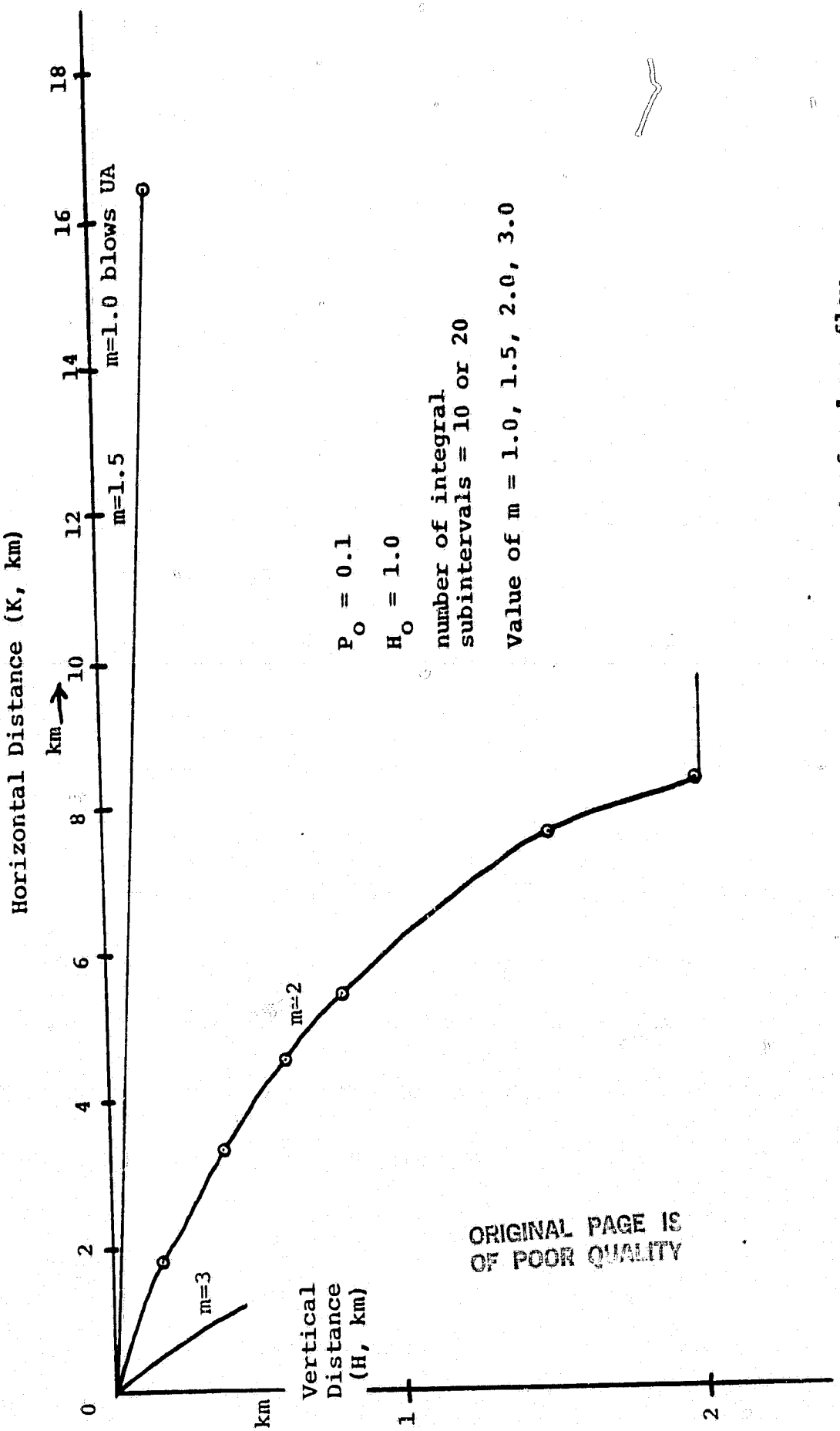

Fig. 3.8 Lava flow bed profiles for steady state retreat of a lava flow eroding a substrate.

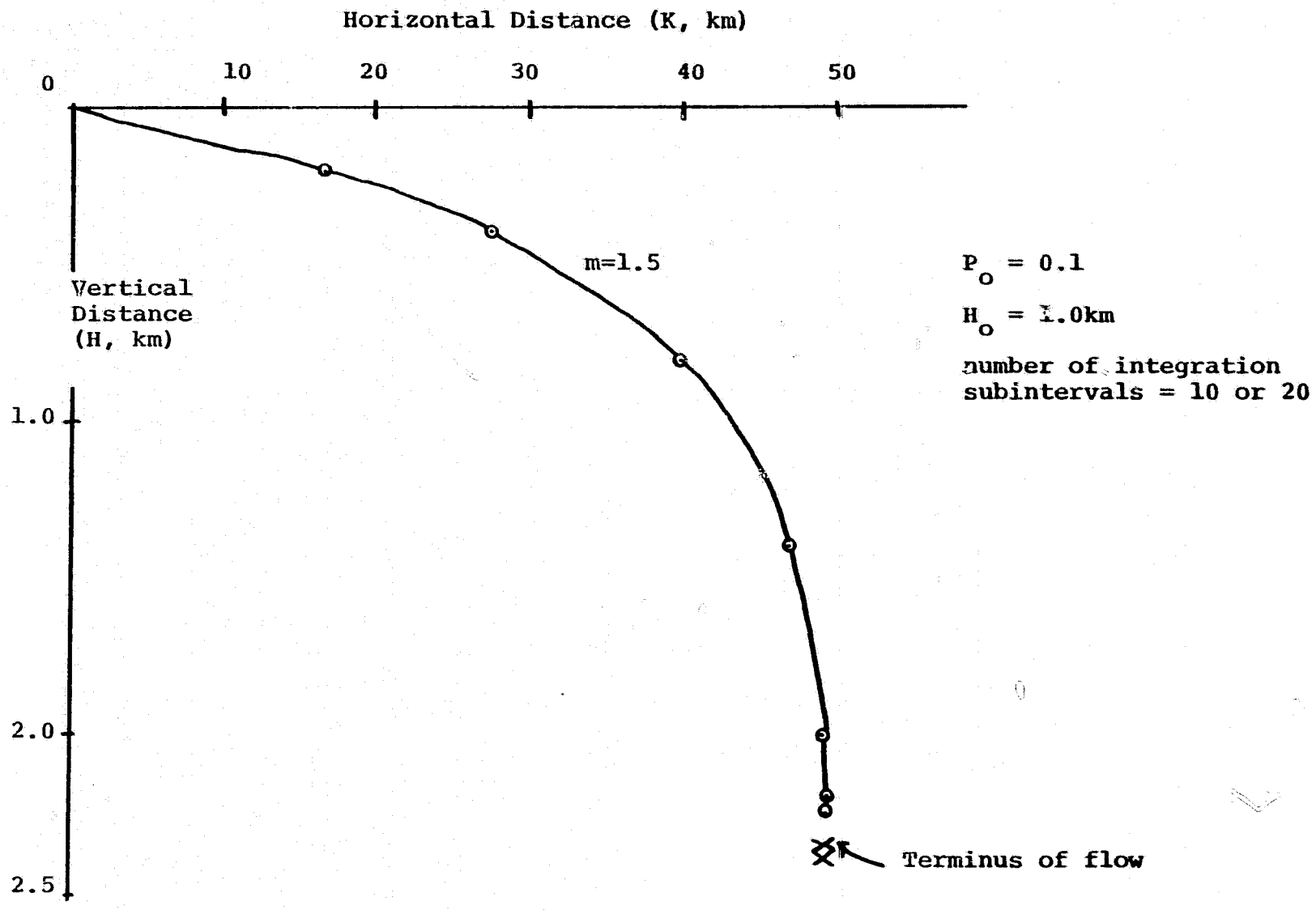

Fig. 3.9 Lava flow bed profiles for steady state retreat of a lava flow eroding a substrate.

References

Bagley, F.J., J.M. Owen, and A.B. Turner, Heat Transfer, 438p., 1972.

Carr, M.H., The Role of Lava Erosion in the Formation of Lunar Rilles and Martian Channels, Icarus, 22, pp. 1-23, 1973.

Hulme, G., The Interpretation of Lava Flow Morphology, Geophys. J. R. Astr. Soc., 39, pp. 361-383, 1970

Hulme, G., The Determination of the Pheological Properties and Refusion Rate of an Olympus Mons Lava, Icarus, 27, pp. 207-213, 1976.

Murase, T. and A.R. McBurney, Viscosity of Lunar Lavas, Science, 167, pp. 1491-1493, 1970.

TASK 4 LAVA EROSION: LABORATORY SIMULATION AND TWO DIMENSIONAL FINITE ELEMENT MODELS

The two aspects of this task were conducted in parallel beginning in June 1979. The laboratory wax model experiments were very limited in scope and were concluded by the middle of August 1979. Development of the two dimensional finite element codes for modelling thermal lava erosion continued up to the end of the contract period.

A. Wax Model Experiments

Beginning in June 1979 we performed a series of experiments simulating lava erosion by physical modelling methods. Prof. Jay Melosh, at that time of Caltech, permitted us to use laboratory facilities set up for conducting physical simulations of ocean floor spreading using hot wax. We allocated some discretionary funding for equipment to investigate the feasibility of simulating lava erosion using hot wax. Mr. José Helú, Prof. Melosh's former research assistant in the Caltech physical modelling experiments, assisted us with these wax model experiments. The results of these experiments exceeded our expectations and proved to be a valuable guide to our theoretical modelling efforts.

1. Experimental Approach

To simulate erosion of rock by a flow of molten lava we pumped hot wax into a channel of rectangular cross sections which had been formed in a wax substrate. The experimental set up is shown in Fig. 4.1 (a) (b). It includes a thermomix

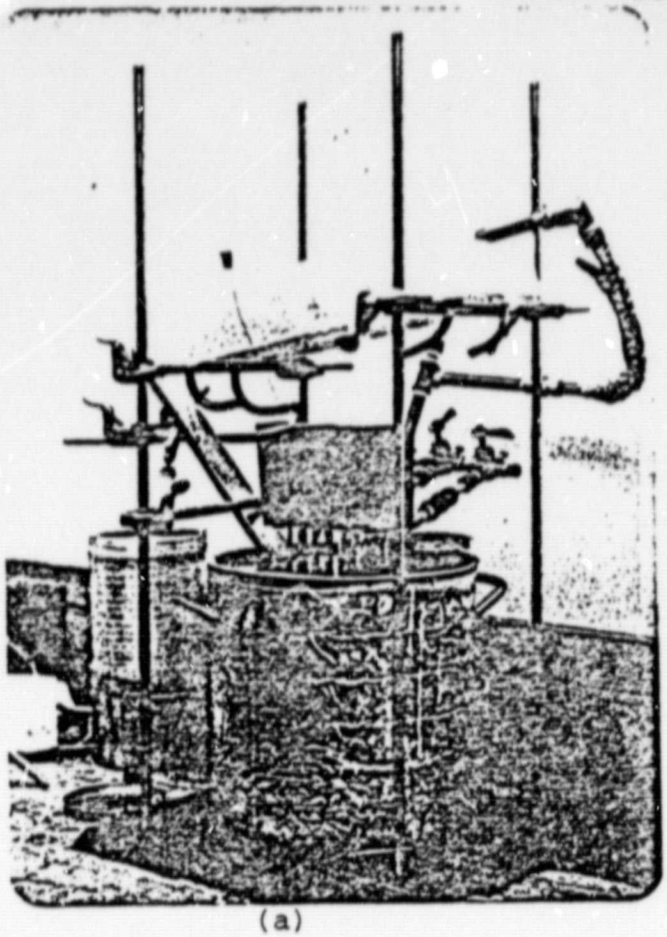

(a)

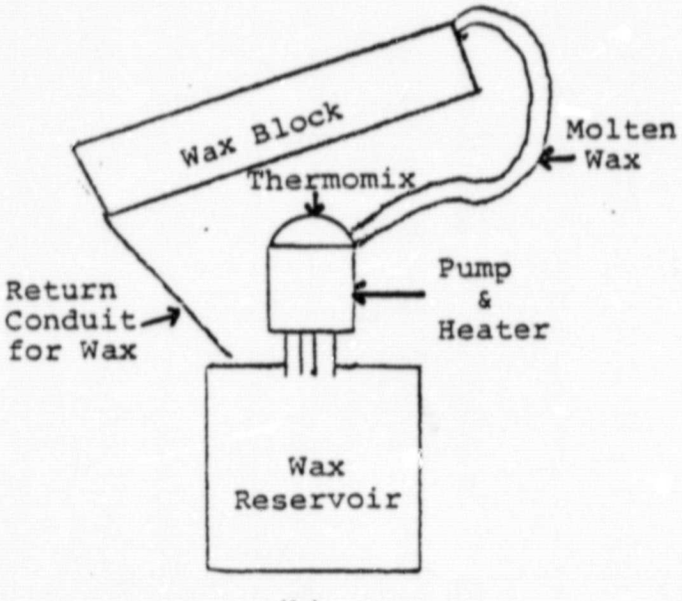

(b)

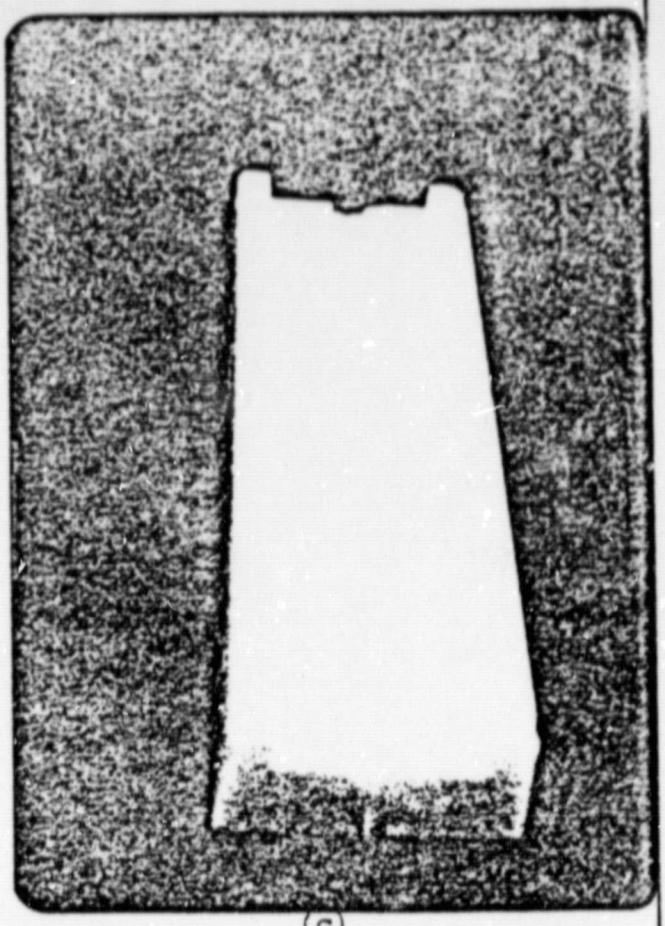

(c)

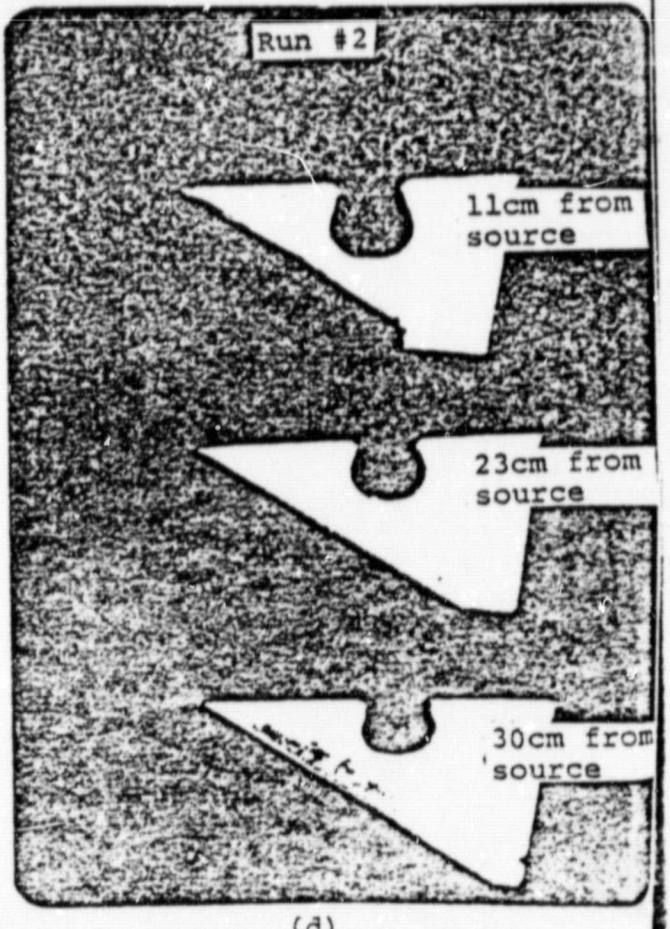

(d)

Figure 4.1

heater to heat the wax to a uniform temperature, a pump to supply the fluid at a uniform rate, a wax casting with a channel of rectangular cross section, and a pump for collecting wax reaching the end of the channel. Two experiments have been conducted so far using polythylene glycol (Carbowax 4000) for the fluid and substrate.

2. Results

Photographs of the wax casting after one experiment are shown in Fig. 4.1(c). In this experiment, material was eroded along the entire length of the channel. At the inlet the hot wax dropped onto the channel floor and this resulted in the formation of a depression; at the outlet hot wax cascaded over the edge of the channel and eroded headward.

An interesting feature of the erosion process is evident in the channel cross sections (Fig. 4.1(d)). There has been significant removal of material by lateral erosion except near the surface of the flow where hot wax has solidified and accreted creating a significant overhang. This behavior was not suggested directly by the theoretical modelling efforts of Carr (1974). However, the forms of the isotherms developed when a hot fluid occupies a cavity of rectangular cross section (Carr, 1974) suggest that thermal erosion will develop more rapidly below the surface of a flow than right at the surface, so in retrospect, the results of the hot wax erosion experiment are not surprising.

The depth of the channel before and after the experiment was measured with a digitizer and the total erosion at the channel center was calculated and plotted for one of the experimental runs (Fig. 4.2). The large amount of erosion near the channel source was a consequence of a 'waterfall' effect created when the hot wax first spurted on to the surface of the channel. Between 10cm and 35cm the amount of erosion declines steadily as the hot wax cooling through transfer of heat to its environment and assimulation of orignal cool wax from the channel wall and floor. Channel sections were also digitized illustrating the variation of erosion and accretion as a function of depth and are displayed in Fig. 4.3)..

In Table 4.1 we have summarized the effects of thermal erosion by the hot fluid wax on the wax substrate. A significant parameter is the transport and erosion efficiency, i.e., the proportion of material that flows out of the channel that is derived by erosion of the substrate. It is most conveniently expressed as the ratio of the volume of material eroded to the volume of material which flowed in the channel. Material removed due to headward retreat at the channel outlet was excluded from this estimate.

The relevance of hot wax simulations to the behavior of lava flows has been considered by Hodgson (1969) (Appendix 4.1) and at a workshop held at the Los Alamos Scientific Laboratory (Widdicombe and McGetchin, 1976). The emphasis was

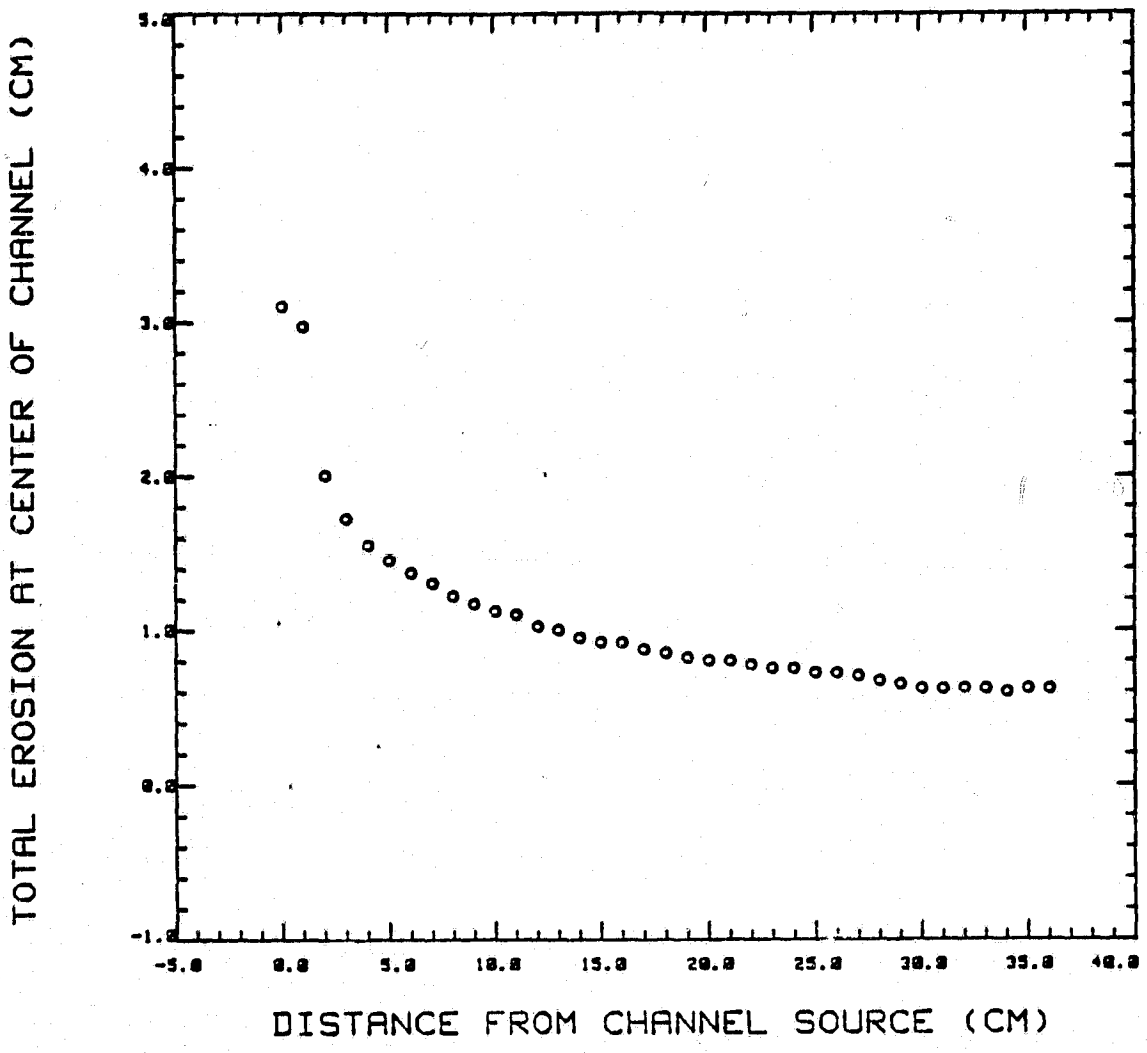
TOTAL EROSION AT CENTER OF CHANNEL (CM)
5.0
4.0
3.0
2.0
1.0
0.0
-1.0
-5.0
0.0
5.0
10.0
15.0
20.0
25.0
30.0
35.0
40.0
DISTANCE FROM CHANNEL SOURCE (CM)
RUN NO. 2 TIME=45 MIN.
73 DEG. CENTIGRADE FLOW RATE=1.3 L/MIN

Figure 4.2

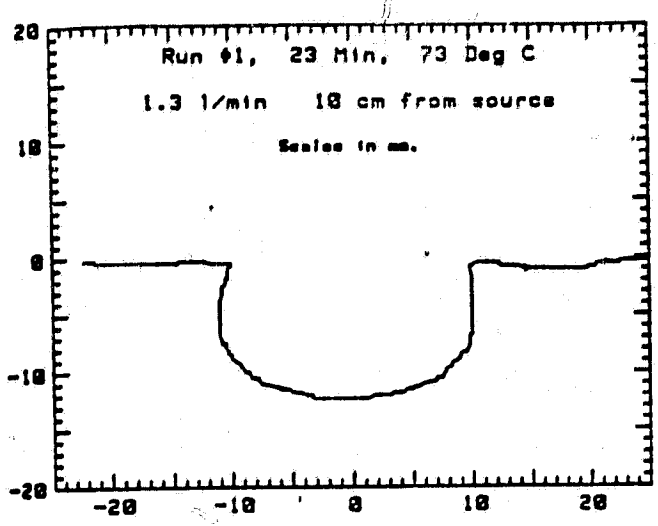

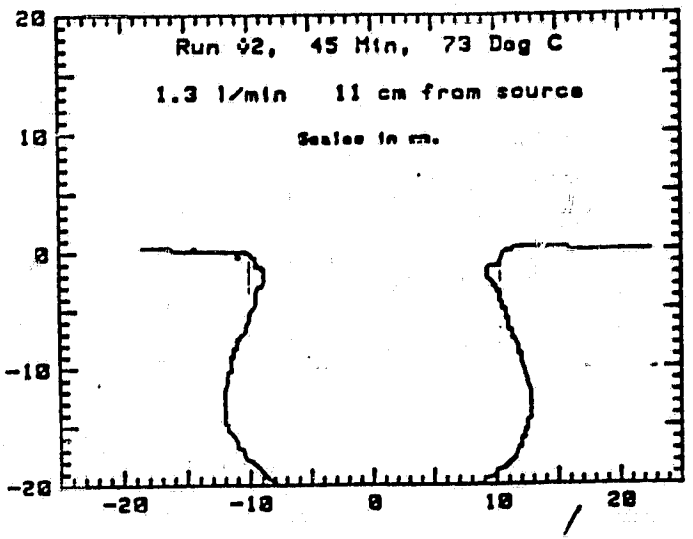

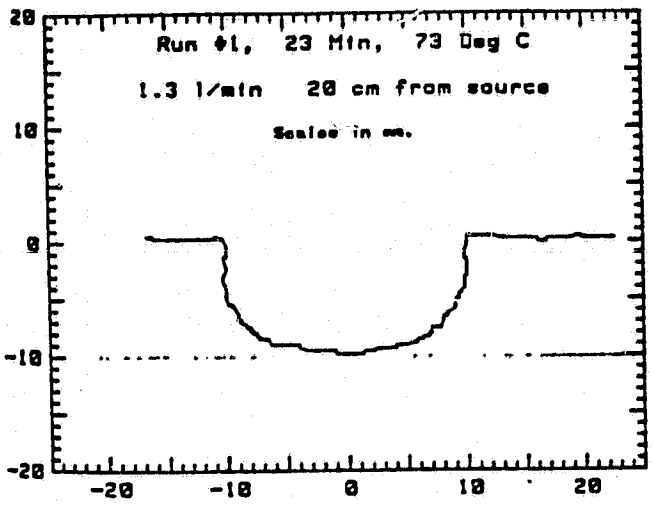

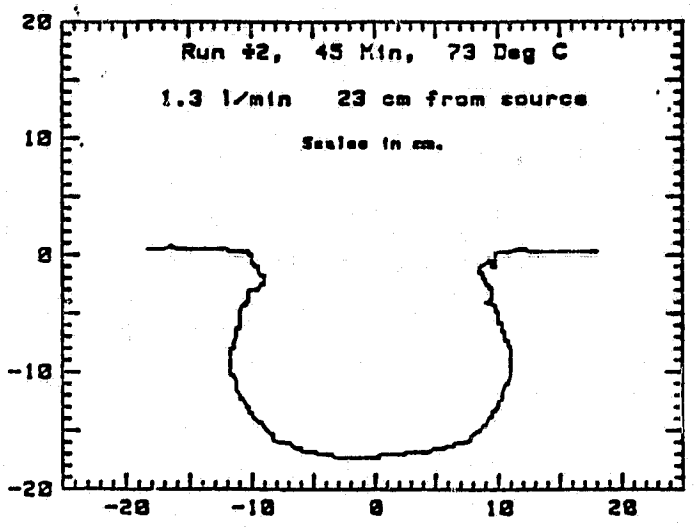

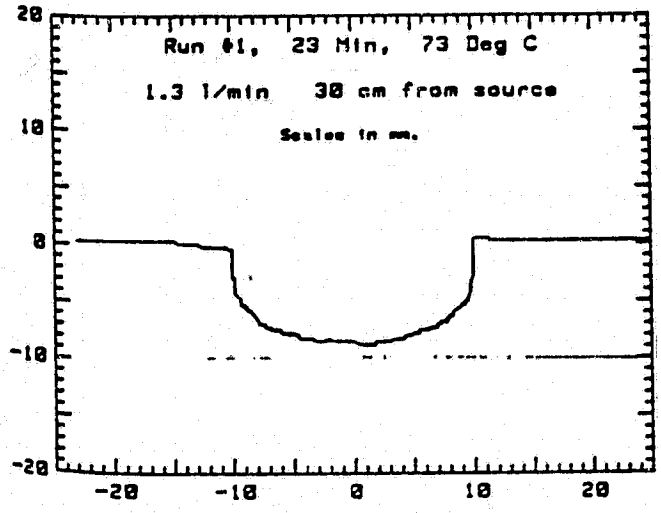

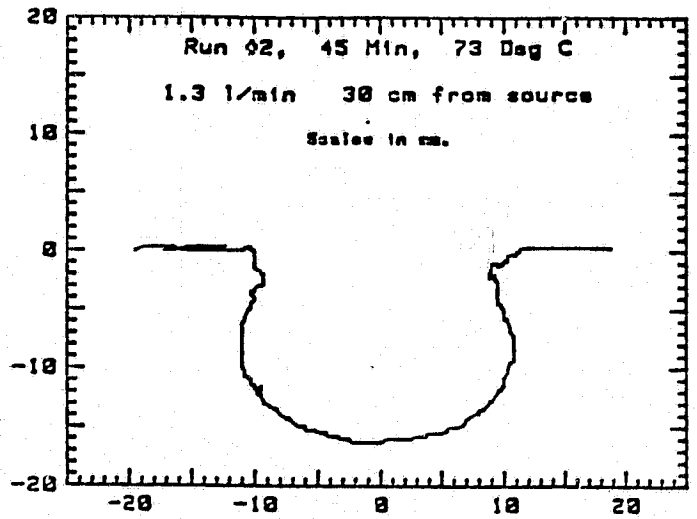

a b

Figure 4.3

TABLE 4.1 DATA ON THERMAL EROSION EXPERIMENTS WITH HOT WAX

Experiment Number	Channel Cross section	Channel Slope (degrees)	Initial Temperature (^{o}C)		Flow Conditions			Erosion[3] Efficiency
			Hot[1] Wax	Substrate[2]	Rate liters/min	Duration (min)	Character	
1	Rectangular Straight	20	73	21	1.30	45	Steady	1.1×10^{-3}
2	Rectangular Straight	20	73	21	1.30	23	Interrupted	2.6×10^{-4}

Notes 1 This hot wax temperature was measured at the pump output. The measured temperature may be 1 or 2^{o} higher than it is where the wax enters the channel.

2 Substrate temperature has beer equated to room temperature. The wax block was not instrumented for temperature measurements.

3 Erosion efficiency is defined here as the ratio of the volume of material eroded to the total volume of the flow.

on the emplacement and mechanics of a flow of lava and not on the erosion of a substrate (substrates which did not melt were used), however, the similitude arguments developed (see Appendix 4.1) are still pertinent here. Thus, the approach of using scaling relationships to describe the results in laboratory experiments should also work with the erosion problem. The wax we used (Carbowax 4000) was the same that was used in experiments for the lava experiment at Los Alamos. It melts to a clear liquid at 55°C, forming a non-Newtonian fluid. Many of the similitude numbers match those for lava (see Appendix 4.1); moreover it does form analogs of lava flow features such as natural levees, lava tubes, and pahoehoe surface textures.

3. Further Investigations

Laboratory experiments with hot wax provide a powerful tool for developing qualitative and quantitative understanding of the mechanism of thermal erosion at a geological scale. Such experiments can be used to validate numerical methods for calculating lava erosion; study thermomechanical erosion in circumstances which are not practical with numerical methods, e.g., pulsed flows, channels of varying cross sections, sinuous channels, and study the formation of morphological and structural features of the lava erosion regime.

Specific goals of future investigations with hot wax models might be:

1) To validate the numerical codes for thermal erosion developed for slab flow and channel flow as described in Task 4B using laboratory experiments with flows of hot wax.
2) To examine the transition from erosional to depositional conditions using the physical modelling approach.
3) To investigate how the efficiency of erosion depends on such parameters as temperature, viscosity and flow rate.
4) To examine the effect of pulsed or intermittent flow on erosion rates in a channel.
5) To examine channel cross section and profile development under a variety of flow conditions.
6) To examine flow in sinuous channels.
7) To apply the validated theoretical codes to the modelling of large scale thermomechanical erosion on planetary surfaces and to investigations of the origin of certain classes of erosional features on planetary surfaces.

An improved experimental set up would be needed to achieve the accuracy and reproducibility needed for meeting these objectives. Equipment additions would be required for:

1) improving control of the flow rate and temperature of the fluid wax entering the wax channel,
2) improving monitoring of the temperature of the wax substrate, and of the fluid wax along the length of the channel,
3) refining measurement of channel profile and cross section,
4) making additional molds to permit more experiments to be run. At present, each mold takes several hours to coool and this limits the number of experiments,
5) use of channels with varying amounts of sinuosity in plan,
6) using channels with obstructions and constrictions.

B. Two-Dimensional Finite Element Models

Our approach to the problem of modelling thermal erosion using finite element techniques involved two stages. First, we spent some time developing a basic understanding of finite element techniques and the stability relationships that restrict their applicability. Then, we embarked upon a serious formulation of the lava erosional problem and developed a series of computer programs of progressively increasing complexity.

1. Modelling Methods

Our initial investigations were designed to gain familiarity with some commonly used finite difference algorithms. We exercised these algorithms on some simple thermal problems and compared the observed convergance properties with those anticipated theoretically.

The vorticity-stream function method was anticipated being used for our numerical investigations of thermal erosion. In this method the momentum equations of Navier Stokes for incompressible flow are cast into the form of a parabolic vorticity transport equation. This equation must be solved for the specified boundary conditions and the solution used as the inhomogeneous term in a Poisson equation for the stream function.

After solving this elliptic problem for the stream function by iterative methods, velocities are obtained as the partial derivatives of the stream function with respect to the spatial coordinates. The vorticity transport equations are identical in form with the heat transport equations and so this approach appears to be attractive for studying thermal erosion where heat and vorticity transport are coupled. In a problem where there is no flow, or where the flow is specified, the solution of the thermal analog of the advective diffusion equation for vorticity transport represents a complete solution to the problem of interest.

Several finite difference schemes were examined for solution of these equations. The Dufort-Frankel leapfrog is a single step, three level finite difference method for solving the advective diffusion equation. This method is unconditionally stable as there is no limitation on the value of the diffusion number ($d = \frac{\alpha \Delta t}{\Delta x^2}$ This means that the mesh size can be reduced without requiring a much larger reduction in the size of the time step. The only stability restriction is the inviscid requirement on the courant number ($C = \frac{\alpha \Delta t}{\Delta x}$) . of $C \leq 1$. We developed a computer program to apply the Dufort-Frankel method to a two-dimensional thermal diffusion problem as described in Appendix 4.2.

With the experience gained in these exercises we were in a position to address the specifics of thermal erosion. In this we benefited from the guidance of Stephen Keihm. Our approach here was to investigate models of progressively increasing complexity. The models are described here below; the computer programs to implement the models are included in Appendix 4.3.

2. Thermal erosion for a plane laminar constant viscosity flow with a yield temperature.

This model resembles the approach originally formulated in a one dimensional form by Carr (1974) in that when the substrate temperature reaches or exceeds the yield temperature the material participates in the flow.

Approach

We first assume the velocity field for a plane, laminar, constant viscosity flow:

$$V(y) = \frac{g}{2\nu} \sin\phi \ (H^2 - y^2) \qquad 4.B.1$$

where H = flow layer thickness

ν = kinemetric viscosity

g = gravity accel.

Then, as a first approximation, with the velocity field given, the problem can be treated from a purely thermal approach. We have used a Forward Time Centered Space (FTCS) algorithm to model the conductive heat flow; heat is advected at the fluid velocity using a Forward Time Forward Space (FTFS) algorithm.

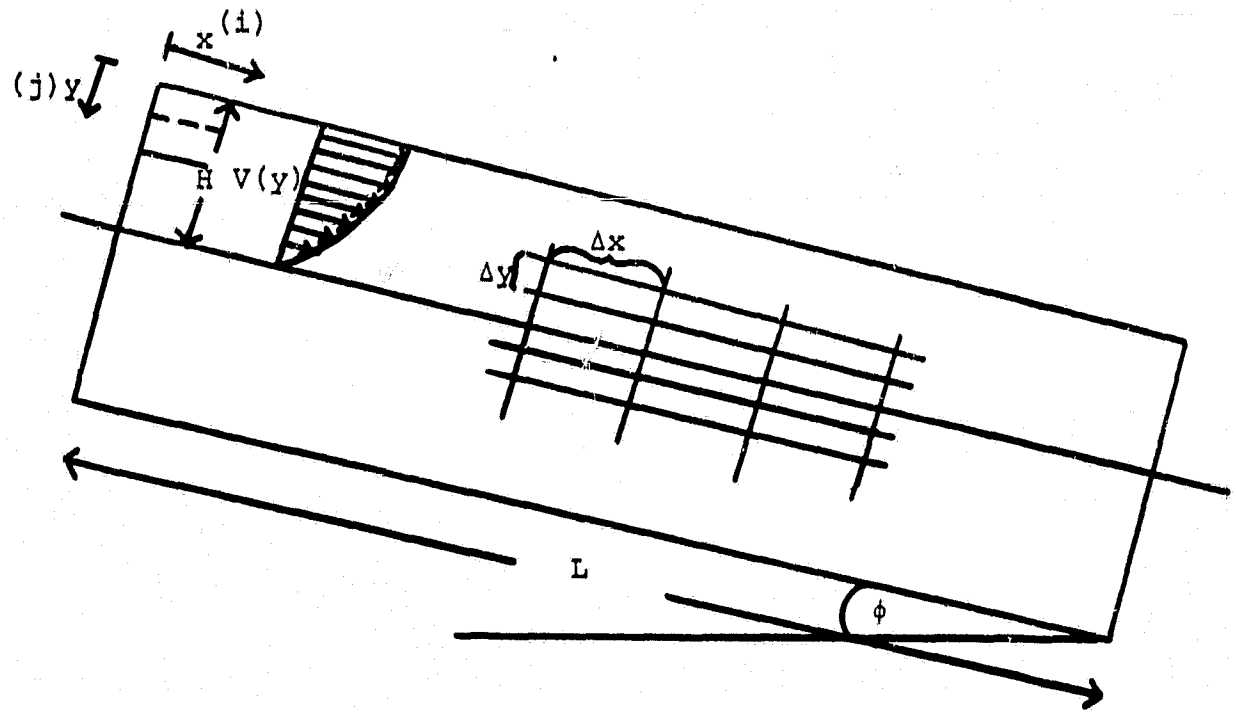

Fig. 4.4 Geometry for Finite Element Simulation of Thermal Erosion.

For the rectangular mesh as shown above

$$\rho C \Delta V \Delta y \frac{T_{i,j}^{n+1} - T_{i,j}^{n}}{\Delta t} = V_{i-1,j} \cdot \Delta y \cdot \rho C \cdot T_{i-1,j} - V_{i,j} \Delta y \rho C - T_{i,j}$$

$$+k \cdot \Delta y \left(\frac{T_{i-1,j} - T_{i,j}}{\Delta x} \right) + k \Delta y \left(\frac{T_{i+1,j} - T_{i,j}}{\Delta x} \right)$$

$$+k \cdot \Delta x \left(\frac{T_{i,j+1} - T_{i,j}}{\Delta y} \right) + k \Delta y \left(\frac{T_{i,j-1} - T_{i,j}}{\Delta y} \right) \qquad 4.B.2$$

But $V_{i-1,j} = V_{i,j}$ since V is indepent of longitudinal direction

$$\frac{T_{i,j}^{n+1} - T_{i,j}^{n}}{\Delta t} = \frac{V_j}{\Delta x} \quad (T_{i-1,j} - T_{i,j}) \qquad 4.B.3$$

$$+ \frac{k}{\Delta_x^2} (T_{i-1,j} - 2T_{i,j} + T_{i+1,j})$$

$$+ \frac{k}{\Delta_y^2} (T_{i,j-1} - 2T_{i,j} + T_{i,j+1})$$

where $v_j = V(y)$ is given above.

Since the velocity field is assumed fixed, the removal of material from the supporting wax layer must be evaluated by a thermal criterion. Two approaches might be used on limiting cases:

1. Evaluate the depth of erosion as a function of the downslope coordinate, x, by fitting the temperature profile of the wax base to a quadratic function. The depth of erosion would then be estimated by the depth to which a 'yielding' temperature, Ty, was attained. This is a similar approach to the one dimensional model with conduction and convection described in Section 3.B.2. This would correspond to a lower limit estimate of the erosion since it does not take into account the gradual removal of material and resultant new 'contact' of underlying base material to the high, flowing fluid temperature.

2. Add a stipulation in the numerical model that as soon as any base reaches the yield temperature, Ty, it is replaced by the adjacent fluid temperature. This is a similar approach to the 'modified' one dimensional model with conduction and convection described in Section 3.B.2. It is also similar to the scheme used by Carr (1974) and should represent an upper limit on the erosion with heat of melting effects neglected. The amount of erosion is again calculated by the depth of the yield temperature in the wax base.

Boundary Conditions

1. Boundary nodes of the wax base radiate to ambient space as do the surface modes of the wax flow.
2. At the source of the wax flow ($x = 0$; $0 \leq y \leq H$) an input ('left to right') flux corresponding to the hot wax temperature is used.
3. At the 'spill end' ($x = L$; $0 \leq y \leq H$), zero conductive flux is assumed.

Since the flow velocity is assumed constant, we start with all nodes for which $y \leq H$ set to the hot wax temperature, with the wax base ambient throughout.

There is an input at the left of T_1, and the output boundary is held at conditions of no heat flow into or out of the boundary, as is the bottom of the solid wax. The top surface radiates at σT^4, but again, no convective or advective heat flow into the boundary is permitted. These conditions are realized by creating a dummy set of values outside the boundary which are set equal to the values on the inside, causing no heat flow across the boundary. The σT^4 condition is dealt with in a separate step. This leaves only the solid-liquid interface to be dealt with.

In earlier test versions, the interface position was held fixed--i.e. irrespective of the temperature, liquid never solidified, and solid never melted. This is somewhat equivalent to having a thin insulating sheet at the interface, and though unrealistic, served to test the algorithm.

The present version allows for melting and solidification in the following manner:

a) A threshold temperature (T_{th}) is defined at which fluid flow will occur.

b) Solidification is assumed to begin at the far end, and erosion is assumed to begin at the near end.

c) If a cell which was in the original fluid regime drops below the threshold, temperature advection is turned off. Further, the heat that would have been advected into the cell (assuming, of course that the cell in front of it is still fluid) is advected straight up into the cell directly above it.

d) If a cell which was in the original solid regime rises above the threshold temperature, the fluid is 'mixed' with the fluid directly above it. This is accomplished by advecting a quantity of heat less than or equal to the amount of heat needed to bring both cells to the same average temperature. It is presently set up to mix completely in one second (100 iterations).

e) The extra heats needed to accomplish this are held in a separate array and added to the cells (or subtracted from them) at the next iteration.

The FORTRAN program for implementing this simulation is reproduced in Appendix .

Results

Three runs of the program were performed with identical parameters excepted for velocity. These runs simulated the effects of a relatively slow moving lava flow (V = 10cm/sec) moderately fact flow (V = 100cm/sec). The parameters used in these runs and the number of iterations performed and plots generated are shown in Table 4.2.

The immediate output of the program was a listing of temperature values on a 12x17 grid of points (eg. Fig. 4.5(a)). More than 200 printouts of this format were generated. In order to better visualize the results of the experiment a graphical representation of the same data as isotherms was generated (eg. Fig. 4.5(b)). by interpolating individual temperature values from the printouts. Only a small number of these plots were generated.

In Fig. 4.6 we show the isotherms for each run at a series of times into the experiment. The horizontal dashed line in each plot represents the original interface between the substrate at 20°C and the fluid at 1300°C . The 600°C isotherm which is the lowest one plotted provides a useful reference to indicate both the flow of heat into the substrate and the progress of erosion of the substrate.

In Run 1, the 600°C isotherm progresses by about one cell into the substrate during the 96.7hr experiment except close to the source where progress is much more rapid. In Run 2, the 600°C isotherm advanced by all sizes into the substrate during the 96.1 hr experiment at the downstream end and by larger amounts nearer the source. In contrast with Run 1, the isotherm maintains a significant slope for the entire length and is not as sharply curved near the source. In Run 3 the 600°C isotherm advanced by 3½ cell sizes into the substrate during the 96.1hr experiment at the downstream end.

TABLE 4.2 PARAMETERS FOR TWO DIMENSIONAL LAVA EROSION SIMULATION

KAPPA = 0.04

ROC = 0.25

H = 0.50

LENGTH = 1.0×10^7

G = 980

ANG = 30

RUN	VMAX (cm/sec)	NO. OF ITERATIONS	NO. OF PRINTOUTS	NO. OF PLOTS	MAX. TIME (HRS)
1	10	87	30	5	96.7
2	100	173	173	5	96.1
3	1000	870	30	4	96.7

ITERATION# 870 96.7 HOURS

	1	2	3	4	5	6	7	8	9	10	11	12
1	1300.00	1297.33	1294.79	1292.35	1290.02	1287.77	1285.61	1283.53	1281.50	1279.54	1277.63	1300.00
2	1300.00	1297.33	1294.79	1292.35	1290.02	1287.77	1285.61	1283.53	1281.50	1279.54	1277.63	1277.63
3	1300.00	1299.88	1299.64	1299.29	1298.83	1298.27	1297.60	1296.83	1295.97	1295.00	1293.94	1293.94
4	1300.00	1299.89	1299.58	1299.06	1298.28	1297.26	1295.98	1294.47	1292.78	1290.80	1288.67	1288.67
5	1300.00	1297.97	1294.49	1289.98	1284.76	1279.07	1273.07	1266.89	1260.62	1254.34	1248.08	1248.08
6	1300.00	1272.92	1249.76	1229.71	1212.16	1196.62	1182.70	1170.12	1158.64	1148.07	1138.26	1138.26
7	1133.55	1133.55	1108.67	1087.43	1069.09	1053.02	1038.82	1026.10	1014.61	1004.12	994.48	994.48
8	1003.00	1003.00	977.52	956.00	937.61	921.68	907.72	895.33	884.22	874.17	864.97	864.97
9	887.80	887.80	862.65	841.61	823.77	808.44	795.11	783.37	772.91	763.49	754.94	754.94
10	739.70	739.70	714.20	694.74	680.81	668.51	658.54	649.68	634.85	626.59	619.14	619.14
11	527.49	527.49	508.33	492.71	479.80	468.96	459.75	451.81	444.87	438.74	433.27	433.27
12	276.26	276.26	264.94	255.90	248.59	242.58	237.57	233.32	229.66	226.51	223.72	223.72
13	93.39	93.39	89.69	86.42	83.55	81.02	78.81	76.87	75.17	73.69	72.38	72.38
14	31.42	31.42	30.19	29.11	28.16	27.34	26.62	26.00	25.46	24.99	24.58	24.58
15	21.10	21.10	21.03	20.99	20.95	20.92	20.90	20.88	20.87	20.86	20.85	20.85
16	20.07	20.07	20.07	20.07	20.06	20.06	20.06	20.06	20.06	20.06	20.06	20.06
17	20.00	20.07	20.07	20.07	20.06	20.06	20.06	20.06	20.06	20.06	20.06	20.00

Fig. 4.5(a) Matrix of temperature values for Run 3 (VMAX = 1000cm/sec) at 96.7 Hrs.

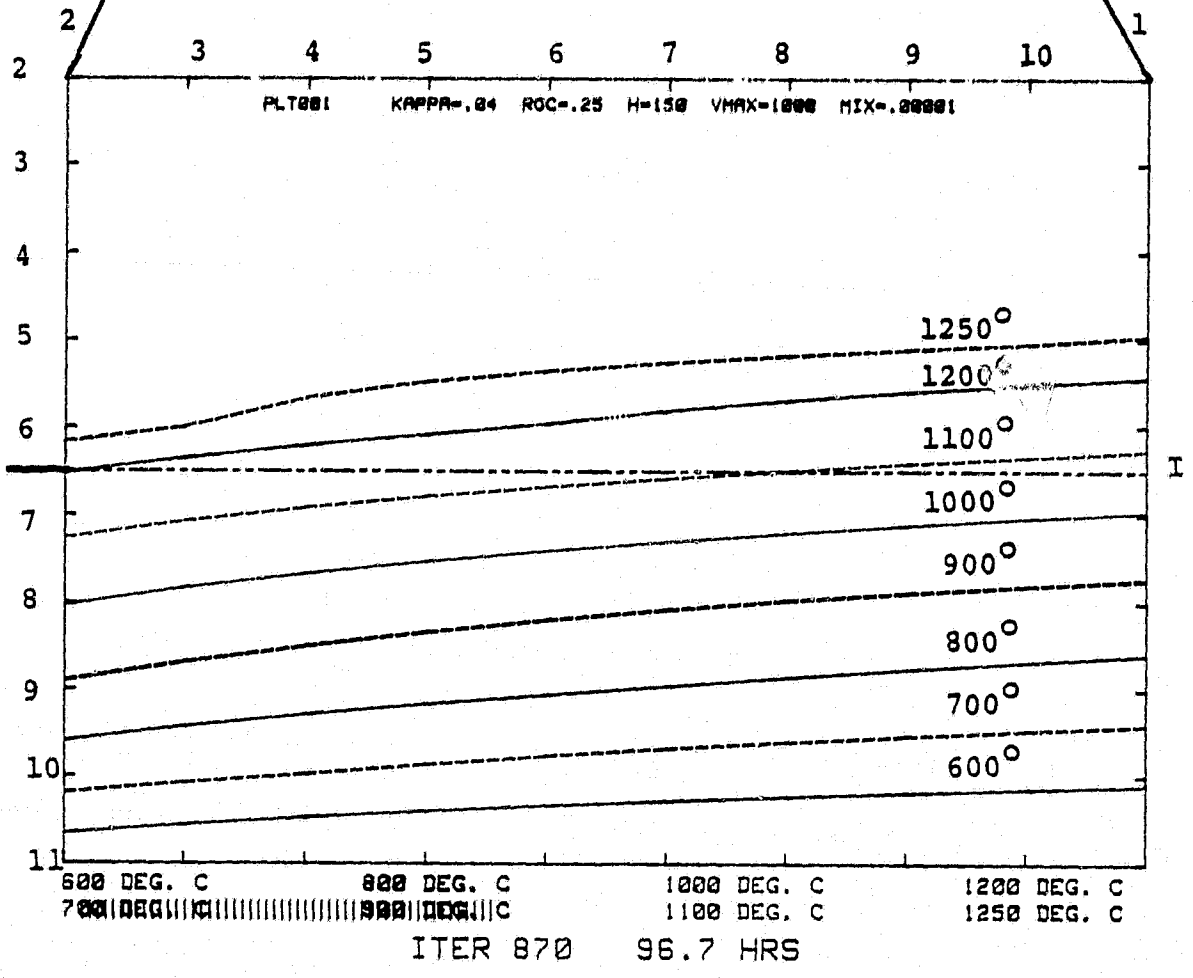

Fig. 4.5(b) Isotherms for data shown in Fig. 4.5(a).

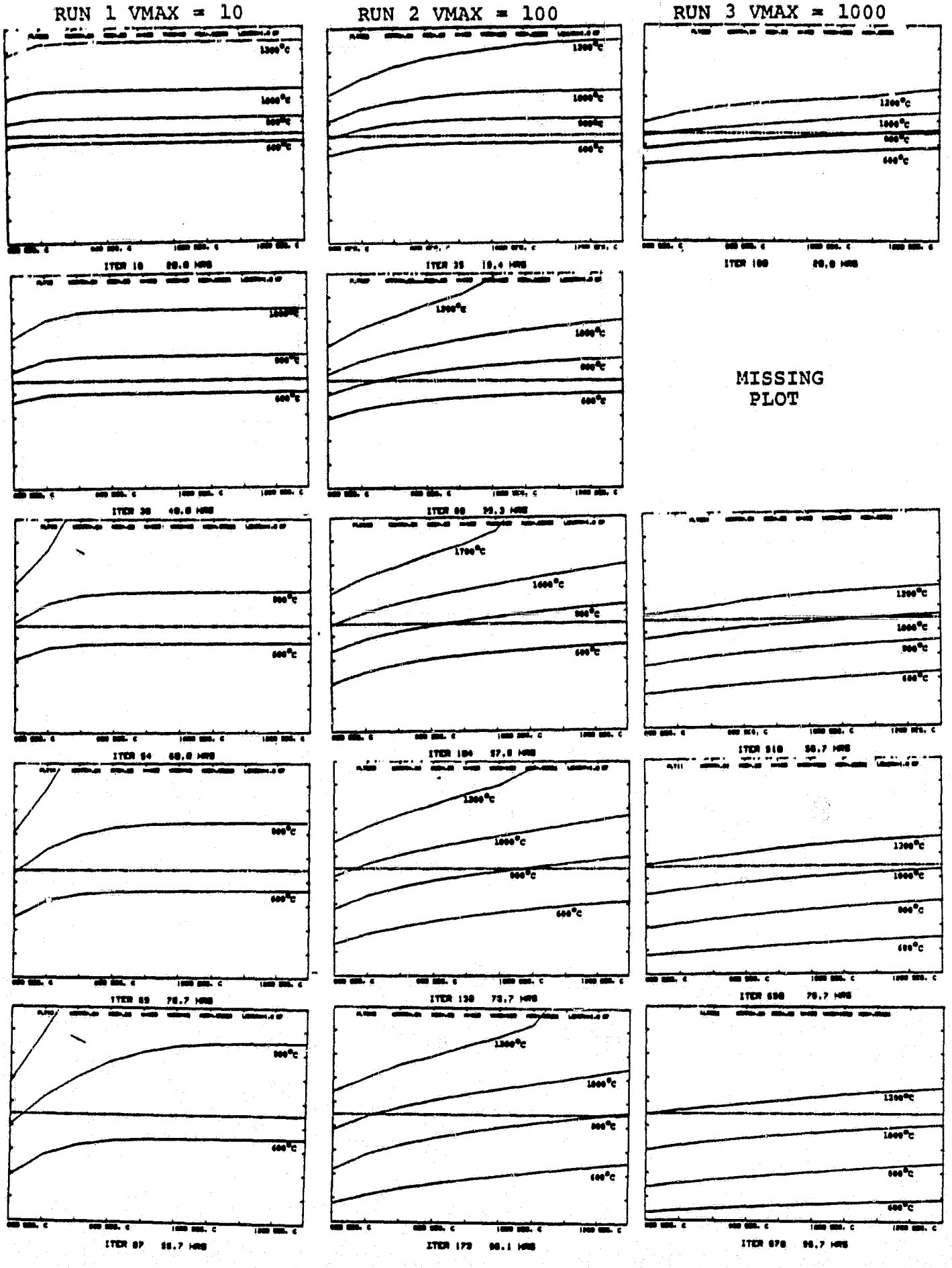

Fig. 4.6 Isotherms for Lava Erosion Simulation

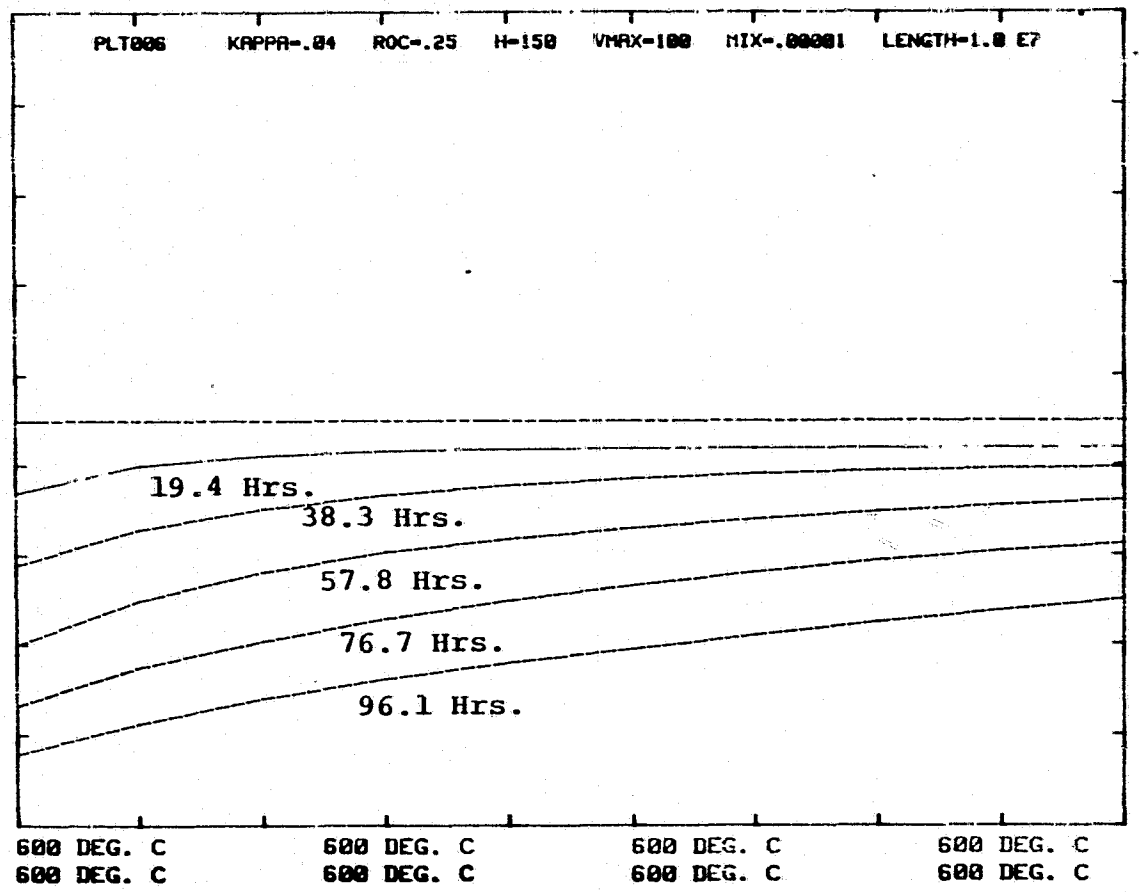

Fig. 4.7 Variation of 600^{o}C isotherm with time for Run 2 (VMAX = 100cm/sec).

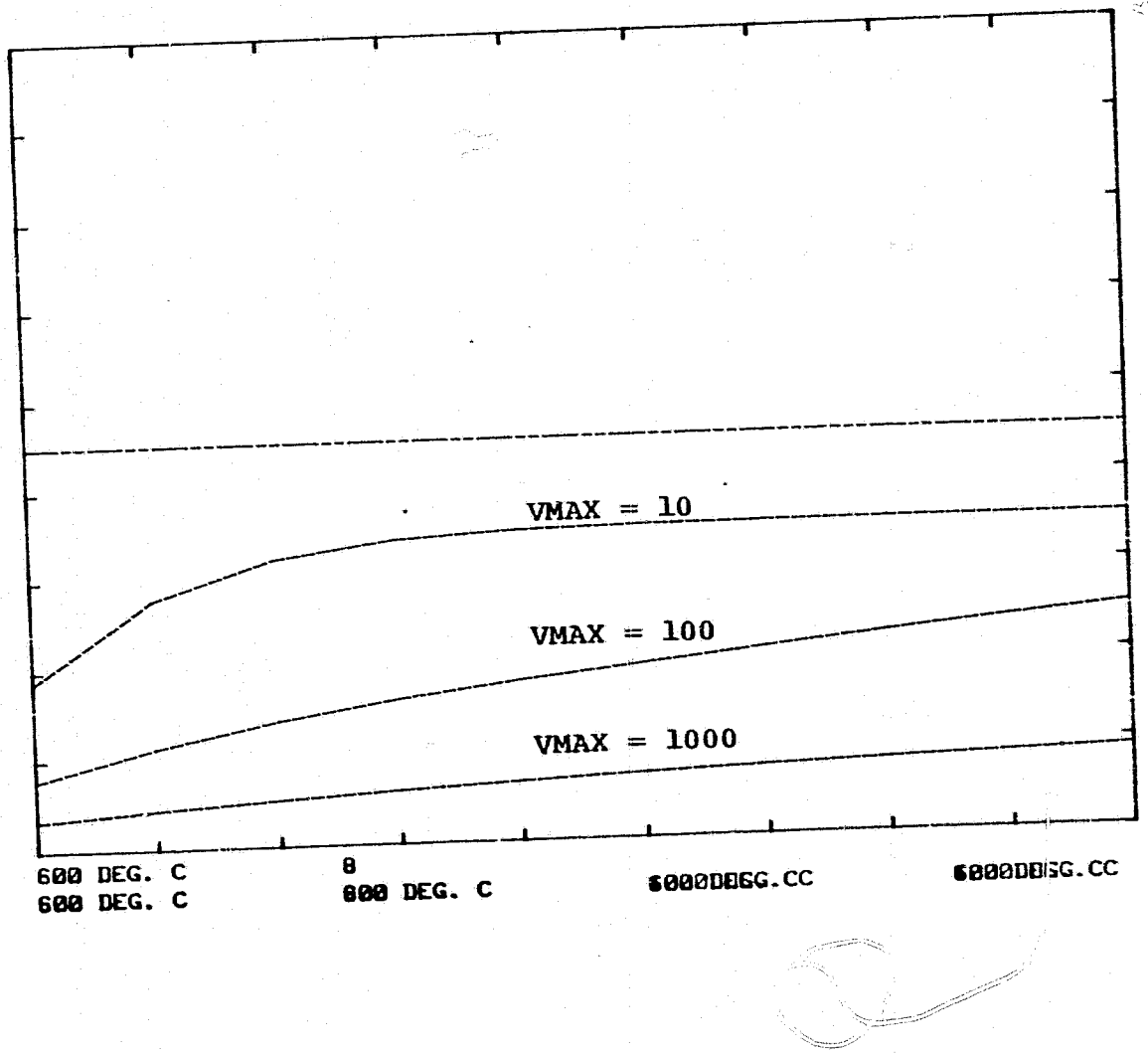

Fig. 4.8 600°C isotherm at 96.7 Hrs. for three different fluid velocities.

CONCLUDING REMARKS

Material from this report is part of a paper which is currently in preparation on the geology of martian rille systems. We envisage that future work on this problem would logically involve a joint experimental/theoretical attack on lava erosion. A proposed follow-on activity submitted in July 1979 (Appendix 4.4) which would have undertaken such a project was not recommended for funding and at this time we have no plans for continuing investigations of this problem.

REFERENCES - TASK 4

Carr, M.H., H. Masursky, W.A. Baum, K.R. Blasius, G.A. Briggs, J.A. Cutts, T.C. Duxbury, R. Greeley, J.E. Guest, B.A. Smith, L.A. Soderblom, J. Veverka, J.B. Wellman. Preliminary Results from the Viking Orbiter Imaging Experiment. Science, 193, 766-776, (1976).

Carr, M.H., The Role of Lava Erosion in the Formation of Lunar Rilles and Martian Channels, Icarus 22, 1-23, (1973).

Cutts, J.A. and K.R. Blasius, The origin of Martian rilles between Lunae Planum and Chryse Planitia (accepted for publication in Icarus) (1978a).

Greeley, R. and J.H. Hyde, Lava tubes of the Cave Basalt, Mount St. Helens, Washington. Geol. Soc. Amer. Bull. 83, 2397-2418, (1972).

Greeley, R., E. Theilig, J.E. Guest, M.H. Carr, H. Masursky and J.A. Cutts, Geology of Chryse Planitia. J. Geophys. Res. 82, 4093-4110, (1977).

Hodgson, G.W., An experimental investigation of simulated lava flows using Carbowax materials, Unpublished thesis, Air Force Instit. Tech., Wright Patterson AFB, Ohio, 119p (1969).

Masursky, H., J.M. Boyce, A.L. Dial, G.G. Schaber and M.E. Strobell, Classification and time of formation of martian channels based on Viking data. J. Geophys. Res. 82, 4016-4038, (1977).

McGetchin, T. and J.R. Smyth, The Mantle of Mars: Some possible geological implications of its high density. Icarus 25, 351-369, (1978).

Schonfeld, E. Martian Volcanism. Abstracts of Eight Lunar Science Conference, Houston, Texas, March 1977.

Widdicombe, R. and T. McGetchin , Summary of workshop on experimental simulation of lava flows, Los Alamos Scientific Laboratory Memorandum LA-UR 761577, March 11, 1976.

APPENDICES TO TASK 3

3.1 Models of Erosion Relevant to Channel Formation on Mars

3.2 Temperature Dependence of Rock Conductivity

3.3 Computer Program to Calculate Temperature Field in a Laminar Flow of Constant Viscosity with Uniform Heat Input at the Base of the Flow

3.4 Comparison of Conditions for Laminar and Turbulent Flow in Several Fluids of Geological Interest

3.5 Computer Program for Computing Equilibrium Slope Profile for Simple Phenomenological Model of Lava Erosion

APPENDICES TO TASK 4

4.1 Abstract of Hodgson (1969) Work on Lava Flow Similitude Using Carbowaxes with Data on Physical Properties of Carbowax and Lava Flows and Model Parameter Values for Wax and Lava

APPENDICES TO TASK 4 (Cont'd)

4.2 Finite Element Modelling Exercises

4.3 FORTRAN Program for two dimensional model of thermal erosion for a plane laminar constant viscosity flow with a yield temperature

4.4 Abstract of Proposal Submitted in July 1979 for Further Investigations of Lava Erosion

APPENDIX 3.1

MODELS OF LAVA EROSION RELEVANT TO CHANNEL FORMATION ON MARS

by

James A. Cutts

Planetary Science Institute
283 S. Lake Ave., Suite 218
Pasadena, California 91101

ABSTRACT

Evidence for the role of lava erosion in the formation of some of the martian channel features between western Chryse Planitia and Lunae Planum is presented. Earlier numerical modelling studies of thermal erosion by lava are reviewed and deficiencies in the model are identified. An alternative simple one-dimensional model is presented which rectifies some of the weaknesses in the earlier model. However, this model also fails to adequately characterize the lava erosional process. The features of more sophisticated numerical models which are needed to fully depict thermal erosion by lava are described. The relevance of these studies to the turbulent regime which may apply in real-world lava erosion are assessed.

For presentation at the
PLANETARY GEOLOGY FIELD CONFERENCE ON BASALTIC VOLCANISM
Snake River Plain, Idaho

Pocatello, Idaho
October 1977

INTRODUCTION

Images obtained by the Viking Orbiter have revealed that many of the so-called martian channels occur in an intimate association with plains vulcanism. These discoveries contrast with the impression provided by the earlier Mariner 9 orbital imagery that the channels were older than the plains units. We have studied a group of such channels in some detail (Fig. 1). The results of this investigation are reported in an article recently submitted to Icarus (Cutts and Blasius, 1977a). The conclusions of that paper are that these channels have been formed by erosion by the overflow of lava from Lunae Planum into Chryse Planitia across the intervening mountainous divide. In this short note, I wish to merely summarize the key points of the evidence bearing on this interpretation and to then report on some recent theoretical examination of the process of lava erosion. Field studies associated with this conference will add some further insights into the mechanism.

EVIDENCE FOR LAVA EROSION BETWEEN LUNAE PLANUM AND WESTERN CHRYSE PLANITIA

Predicting precisely what a large lava erosional channel would look like involves some detailed morphological arguments which are too complex to repeat here. There are two key pieces of information however, which support lava erosion origin for the channels.

1. The channels connect two surfaces which are identified as volcanic plains by conventional photogeologic criteria.
2. The ages of these channels determined by two largely independent methods - small crater density and large crater superposition/ intersection relationships - are indistinguishable from the ages of the adjacent plains. The first method yields an age differential

of less than 0.22 at the 95% confidence level; the second method an age differential of less than 0.24 at the 95% confidence level.

Penecontemporaneity in age supports a volcanic origin for the rilles through two different lines of argument. Firstly, it is a necessary condition for both plains and rilles to have been formed by lava. Secondly, it requires a remarkable coincidence for an erosional episode involving some other high density flowing medium to have occurred just once in Mars history and almost contemporaneously with the effusion of plains basalts.

LAVA EROSION MECHANISMS

The importance of lava erosion as a possible agent of valley formation on lunar and planetary surfaces has been stressed by Carr (1974). Greeley and Hyde (1972) have described field evidence for lava erosion on the earth. Carr (1974) has attempted to model the process of lava erosion in a laminar flow of lava.

Stimulated by Carr's investigations we have attempted to understand the mechanism of lava erosion in more detail. We have re-examined his model and found certain deficiencies. We have performed some preliminary calculations of our own in an attempt to improve the model. However, we have concluded that the problem is such that only a full three dimensional treatment can accurately protray erosional phenomena in a lava channel although significant insights can be gained into the lava erosion process by two-dimensional models of a planar flow in which one dimension is along the axis of flow. Neither CArr's model nor our first-order model incorporate this dimension.

Carr's model of the mechanism of lava erosion

The only detailed investigation of a mechanism of lava erosion that

has been reported is the work of Carr (1974). Mechanical and thermal effects both occur in lava erosion, but only thermal erosion is amenable to mathematical modelling. At the base of a lava flow, where the downcutting process takes place, thermal effects will dominate mechanical effects, since the floors of lava tubes are smooth and glazed providing little opportunity for mechanical plucking.

Carr (1974) has considered thermal erosion as a three step process: first, the wall is heated, then it flows, finally it becomes incorporated in the lava stream. Carr asserts that the first stage operates independently of whether the flow is turbulent or laminar. The second stage, flowage of the walls, depends on viscosity and tangential stress. The viscosity depends only on the temperature in the walls; the tangential stress only on the stream depth for both laminar and turbulent flow. If turbulence is a factor, then it controls incorporation of the flowing wall materials into the stream.

The lava erosive mechanism has been modelled by Carr in order to estimate erosion rates. He assumes that a lava channel grows by heating of its wall materials until they reach a yield temperature (Ty) at which time they become sufficiently fluid to flow and become part of the lava stream. He determines the temperature in the vicinity of a lava channel by using the two dimensional heat equation which he solves by applying a standard relaxation technique to a variably sized array of points representing temperatures in a cross section through the channel and its surroundings. As a starting point, the dimensions of the channel are defined, all points within the channel are set at the lava temperature and the rest of the points are set at $0^{\circ}C$. Two further conditions are that the surface except for the channel is kept at $0^{\circ}C$ and that when any temperature reaches a yield temperature it is replaced by the lava temperature. This second condition implies that

wall material reaching the temperature Ty becomes incorporated into the lava stream.

Calculations made with this model suggest that thermal erosion rates are very sensitive to the difference between the lava temperature and the yield temperature. For temperature differences between 0°C and 100°C the erosion rates vary from zero to approximately one meter per month. However, increasing the temperature difference by a further 200°C does no more than quadruple the erosion rate to approximately one meter per week (Fig.2)

These results, although certainly within the reange of erosion rates that can be observed in nature, may contain serious errors because of deficiencies in the model. These deficiencies occur in three areas: in the representation of the temperature-velocity field at the base of the flow; in the characterization of the temperature and stress dependent viscous properties; and in the algorithm which models the thermal erosion process. The deficiencies are a consequence of achieving mathematical and computational tractability with a 2-D model of channel flow.

The first two problems with the model are coupled. Rather than solve the modified Navier-Stokes equations for velocity and temperature, this complex problem of interacting velocity and temperature fields was simplified by separating the transport of mass from the transport of heat. To effect this simplification it was necessary to assume that the material in the substrate of the flow abruptly undergoes a transition from a rigid solid to a mobile fluid at a yield temperature Ty. However, laboratory and field measurements on molten lava as Carr discusses, reveal a gradual, rather than an abrupt change from a rigid solid to a mobile fluid over a temperature range of up to several hundred degrees. There may be materials or circumstances for which this yield temperature is a valid approximation but this has not been demonstrated so we believe some skepticism is justified.

An even more serious difficulty arises with the algorithm that is used to calculate erosion rates from the propagation time of a temperature wave into the channel wall. While this algorithm is only applicable to the yield-temperature formulation of lava properties it appears to give misleading results even with substances for which this yield temperature model is a valid approximation. As we shall now show, the rates of erosion predicted are critically dependent upon the characteristic dimensions of the array of points used in the numerical solution for the propagation of temperature into the channel wall.

Let the array of points upon which temperatures are represented have a characteristic separation δ_{xi} at the channel wall when the i^{th} cycle of iterations, which results in an erosional event, takes place. The time δti for the temperature at the first array point inside the channel wall to reach the yield temperature, thereby bringing about this i^{th} erosional event, will scale as the square of the array separation.

$$\delta ti = Ki\, \delta_{xi}^{2} \tag{1}$$

where Ki is some function of the thermophysical properties of the medium and the thermal conditions at the onset of this i^{th} cycle.

The total time t_n for the yield temperature to propagate successively past n array points is an arithmetic sum of the ti.

$$t_n = \sum_{i=1}^{n} \delta ti \tag{2}$$

and it will propagate a total distance x_n representing the total amount of wall material eroded given by

$$x_n = \sum_{i=1}^{n} \delta xi \tag{3}$$

To find the behavior of tn as the array separations become infinitesimally small, we can assume that all of the δxi and all of the Ki are of the same order as one another. Then substituting in equations (2) and (3) we find that

$$t_n \sim \overline{Ki} \cdot \delta \overline{xi} \cdot xn \qquad (4)$$

Thus, the time to erode a given thickness of channel floor depends on the characteristic array separation which is a mathematical artifact designed to aid in the solution. Moreover, as the array separation tends to zero, which should lead to improved precision in the solution, the time to erode the same thickness of channel floor tends to zero also. It appears that erosion times calculated by the model may therefore be largely an artifact of the particular grid separations chosen.

We consider that to achieve realistic estimates of the rates of lava erosion it is necessary to explicitly consider variations in temperature and velocity in the flow direction as well as perpendicular to it. As a full 3-dimensional treatment becomes extremely elaborate and costly, an alternative is the study of planar rather than channel flows. This will illuminate the basic physics at the base of the flow and will also provide useful, better than order of magnitude, estimates of erosion rates given that effects of channel walls must be ignored. It is probably that estimates of parameter interrelationships will be accurate to a factor of 2.

Not only would a 2-D planar flow treatment yield valid erosion rates but it also may yield numerical results that can be compared with dimensional information on lunar features formed by lava erosion such as topographic profiles along lunar rilles and, excavated volumes of lunar rilles. The important transitional region between lava erosion and accretion could also

be studied. However, some problems such as channel profile and sinuosity would obviously be beyond the range of applicability of the planar flow treatment.

An alternative model of lava erosion (Model 2)

We have made some exploratory calculations of temperature and velocity fields within planar flows. In one set of calculations, detailed below, we studied the flow in the substrate beneath a planar lava flow assuming the relationship between viscosity and temperature for lunar rocks given by Cukierman (1973). It represents another approach to the erosional problem by Carr (1974) but we emphasize that it suffers the same fundamental problem of ignoring the downstream dimension. We adopted an essentially arbitrary criterion for the depth of erosion, namely that depth at which the flow velocity exceeds 10 cm/sec. Our initial objective was to determine the rate of erosion, i.e., the variation of this depth of erosion with time. It proves fruitful to consider separately the dynamic behavior of the lava flow and that of the rock substrate. In the only numerical simulation completed to data: we have considered a steady state flow of an isothermal lava with infinite heat capacity and conductivity over an inclined rock substrate, focusing on the behavior of the rock substrate. Temperature and viscosity versus time profiles for the rock substrate were developed. From these profiles, the rate at which melting rock joins the flow, and hence how the depth of melting increases with time have been determined.

The motion of the substrate beneath a planar lava flow was modelled adopting a simple functional relationship between the viscosity of the substrate and its temperature. We assume that the lava channel grows by heating of the substrate such that the substrate mobilizes and begins to flow in the direction of the lava stream. This flow is assumed to be laminar and the substrate is assumed not to mix turbulently with the free lava stream. However, in

order to simplify the problem we must also take the lava flow to be an isothermal reservoir of heat at temperature T_L. As we are concerned only with the behavior at the base of the flow, a one dimensional solution for a planar rather than a channel flow is adequate to expose the basic physics of what happens in a channel flow (Fig. 2).

As a starting point we assume that the temperature of the substrate is To and the thermal diffusivity is K. At time t=0 an insulating layer separating the lava from the substrate is removed bringing the two into thermal contact. The temperature within the substrate has a straightforward analytic solution if K is independent of temperature. Thermal diffusivities of silicate materials in fact, show considerable variation (a factor of 10) over the temperature ranges in question but we will ignore this complexity in this treatment. Thus:

$$T_s = (T_L - T_{so}\left[1 - \mathrm{erf}\left(\frac{y}{2}\sqrt{\frac{1}{Kt}}\right)\right] \qquad (5)$$

The viscosities of lunar basalts vary from perfect rigidity on time scales relevant to the duration of a lava flow, near or below 900°C to approaching the consistency of motor oil, at 1200°C. We have performed a parameterization of data by Cukierman et al., (1973) for the viscosity(η) of a basalt which is considered here to form the bed or substrate of a channel flow.

$$\log \eta = A + B/T + C/T^2 \qquad (6)$$

where A = 3.145

B = -1.84×10^4

C = 37×10^7

The temperature within the substrate will vary sufficiently slowly for inertial effects to be neglected. Consequently the equation of motion for the fluid is:

$$\frac{d\tau_{xy}}{dy} = \frac{d}{dy}\left(\eta \frac{du}{dy}\right) \tag{7}$$

Integrating,

$$\tau = (h\rho_L + y\rho_s)\, g \sin\theta = \eta \frac{du}{dy} \tag{8}$$

where y = depth below lava/substrate interface

u(y) = velocity of substrate parallel to interface

$\eta(y)$ = viscosity

h = depth of lava

ρ_L = density of lava

ρ_s = density of substrate

g = acceleration of gravity

θ = slope magnitude

A solution consistent with the boundary equation can be obtained by integrating (8)

$$u = \int_{\infty}^{y} \frac{du}{dy}\, dy = \int_{\infty}^{y} \frac{1}{\eta}(h\rho_L + y\rho_s)\, g \sin\theta\, dy \tag{9}$$

The rate of flow along the channel is estimated by integrating (9)

$$R = \int_{\infty}^{0} \left[\int_{\infty}^{y} \frac{du}{dy}\, dy\right] dy \tag{10}$$

Numerical solutions for the flow rate as a function of time have been obtained with a computer program (Table 1) and are shown for a variety of lava temperatures in Fig. 4. The

figure clearly illustrates how the substrate flow builds with time. The semi-infinite character of the boundary conditions results in no net removal of substrate material. For an estimate of the deepening of the channel produced when all the lava flow is drained we have somewhat artificially taken the 10 cm/sec velocity level as the base of the flow. Figure 5 illustrates how this level changes with time.

Our results, identified as Model 2, are compared with the thermal erosion data obtained by Carr in Figure 2. Also shown is the viscosity-temperature relaionship used in our calculations. Model 2 must overestimate the time required to remove one meter of substrate as it incorporates no means of bringing fresh hot lava into contact with the substrate. However, we emphasize that we consider neither erosion rate vs. temperature relationship in Fig. 2 is valid because of the inadequacies of both models.

DISCUSSION

Although the calculations made above illustrate how the viscous properties of the substrate rocks can be brought into the assessment of flow processes occurring during lava erosion, they do not permit a meaningful calculation of erosion rates and they provide no insights into the changing character of the flow regime along the channel. In order to do this it is necessary to set up a 2-dimensional model treating the temperature and velocity fields in both the lava flow and the substrate and taking convective as well as conductive heat transfer into account.

The goals of such an investigation would be fourfold:

1. To determine rates of lava erosion with realistic numerical models of heat and mass transfer processes in the bed of a planar lava flow.

2. To estimate the efficiency of lava erosion (the ratio of eroded material to flow material) as a function of slope, viscosity and substrate material properties.

3. To examine the temporal evolution of the profile of the bed of a planar lava flow due to lava erosion as a function of the initial profile, the properties of the eroding flow and the properties of the substrate.

4. To study the transition between lava erosion and lava accretion as a function of slope profile, the properties of the lava flow, and the properties of the substrate.

The geometry of the model for simulating lava erosion of an inclined substrate by a planar flow is depicted in Fig. 5. Heat and mass transfer between and within the flow and the substrate would be modelled using the general equation of heat transfer (Landau and Lifshitz, 1959, p. 185) modified to handle temperature-dependent viscosity (Bayley, et al., 1975). Thermodynamic and kinetic variables would be computed on an array of points within the flow materials and within the substrate.

Initially, the substrate is assumed to have a uniform temperature Tso and the lava flow a uniform temperature T_{Lo}; they are assumed not to have been previously in thermal contact. Initial velocities are zero in the substrate, uniform and non-zero in the lava at a rate appropriate to the constant viscosity and the slope.

At t=0, heat excahnged is initiated across the half-plane downstream of a central reference point. This artifice permits investigation of the profile of lava erosion peculiar to the origin of the flow as well as the more gradually changing gradients for downstream. Initially only conduction is significant but as the thermodynamic structure of the flow field evolves, convective transfer will become more significant in heating they substrate.

Experimentally determined data on lunar rocks would be used for the thermophysical properties of the lava flows and substrate. Some of these parameters such as viscosity and thermal diffusivity are temperature dependent. To more precisely express the phenomena of flow in geologic

materials, a form of plastic flow model is needed such as the Bingham fluid, in which the deviatoric strain rate is proportioned to the deviatoric stress difference in excess of a chosen yield stress.

How relevant are investigations such as these when real lava erosion problems involve channel flow not planar flow and turbulence is likely to play an important part in the erosion process? The same response suffices to answer both questions. The 'action' in thermal lava erosion, as far as the basic issues of incising channels into a cold rocky substrate is concerned, takes place at the base of the flow. For modelling this interaction in a channel the planar flow model is quite adequate for providing initial insights even though it requires modification for accurate estimation. At the base of the flow also, turbulent effects are at a minimum. Certainly it is necessary to understand the role of turbulence in channel formation as it certainly has an impact. But we first of all need to understand the processes that occur in less complex flow regimes.

SUMMARY

Possible lava erosional channels on Mars have been described. Existing work on the modelling of lava erosion has been reviewed and future directions for numerical modelling studies of lava erosion have been identified. Field studies of prehistoric lava erosional features such as those present in the Snake River plain will provide important insights into the process of lava erosion on lunar and planetary surfaces.

REFERENCES

M. H. Carr, 1974, Icarus 22, 1-23.

J.A. Cutts and K. R. Blasius, 1977, submitted to Icarus.

R. Greeley, 1971a, Oregon Dep. Geol. Mineral Ind. Bull. 71.

R. Greeley, 1971b, The Moon 3, 207-233.

Landau and Lifshitz, 1959, Fluid Dynamics, Addison-Wesley

D.A. Swanson, 1973, Geol. Soc. Amer. Bull., 84, 615-626.

R. Greeley and S.H. Hyde, 1972, Geol. Soc. Amer. Bull. 83, 2397-2418.

Gukierman, 1973.

TABLE 1 (a)

PROGRAM FLOW 73/74 OPT=1 FTN 4.5+414 03/09/77 15.40.22 PAGE 1

```
      PROGRAM FLOW(INPUT,OUTPUT,TAPE6=INPUT,TAPE5=OUTPUT)
      EXTERNAL FMU,FMUX
      COMMON TO,W,T
      NAMELIST/DATA/D,G,PHI,RHOB,RHOL,TO,COND
      READ(5,DATA)
      R=RHOB*G*SIN(PHI)
      S=RHOL*G*D*SIN(PHI)
      DO 300 I=1,6
      TIME=10**(4+I)
      DO 250 K=1,25
      TO=770+10*K
      W=.5*SQRT(1/(COND*TIME))
      SUM=0
      DO 200 J=1,50
      GO TO(10,10,20,20,30,30)I
   10 A=-50.0
      M=1
      B=-J
      GO TO 40
   20 A=-250.0
      M=5
      B=-5*J
      GO TO 40
   30 A=-2500.0
      M=50
      B=-50*J
      GO TO 40
   40 AERR=0
      RERR=1.0E-4
      ZA=DCADRE(FMU,A,B,AERR,RERR,ERROR,IER)
      ZA=S*ZA
      ZB=DCADRE(FMUX,A,B,AERR,RERR,ERROR,IER)
      ZB=R*ZB
      Z=ZA+ZB
      SUM=SUM+Z
      X=B
      Y=FMU(X)
      XFLOW=RHOB*SUM*M
      WRITE(5,100)X,TO,TIME,T,Y,Z,XFLOW
  100 FORMAT(1X,2HX=,F8.1,1X,3HTO=,F6.1,1X,5HTIME=,E8.1,1X,5HTEMP=,F6.1,
     1       1X,4HFMU=,E9.2,1X,2HV=,E9.2,1X,6HXFLOW=,E9.3)
  200 CONTINUE
  250 CONTINUE
  300 CONTINUE
      END
```

SYMBOLIC REFERENCE MAP (R=1)

ENTRY POINTS
4111 FLOW

ORIGINAL PAGE IS
OF POOR QUALITY

TABLE 1(b)

```
      FUNCTION FMUX        73/74   OPT=1                FTN 4.5+414        08/09/7?  15.40.22        PAGE    1

                      FUNCTION FMUX(X)
                      COMMON TO,W,T
                      V=W*X
                      CALL MERF(V,ERF)
                      T=TO*(1+ERF)
                      IF(T-725)10,10,20
              10      FMUX=0
                      RETURN
              20      FMUX=X/(1230.27*10**(2.7*10**7/(T+273)**2-1.84*10**4/(T+273)))
                      RETURN
                      END
```

Handwritten note beside the first lines: Calculates FMUX = X/Dynamic viscosity; this function is also required by DC+PLE" in the calculation of flow velocity.

```
     SYMBOLIC REFERENCE MAP (R=1)

ENTRY POINTS
   4  FMUX

VARIABLES      SN  TYPE          RELOCATION
  46  ERF          REAL                               44  FMUX        REAL
   2  T            REAL             / /                0  TO          REAL          / /
  45  V            REAL                                1  W           REAL          / /
   0  X            REAL               F.P.

EXTERNALS          TYPE    ARGS
      MERF                   2

STATEMENT LABELS
   0  10           INACTIVE                    20  20

COMMON BLOCKS   LENGTH
     / /           3

STATISTICS
  PROGRAM LENGTH                  47B       39
  CM BLANK COMMON LENGTH          3B         3
```

TABLE I(c)

```
      FUNCTION FMU          73/74   OPT=1                   FTN 4.5+414        08/09/77  15.40.22        PAGE    1

 1                    FUNCTION FMU(X)
                      COMMON TO,W,T
                      V=W*X
                      CALL MERF(V,ERF)
 5                    T=TO*(1+ERF)
                      IF(T-725)10,10,20
               10     FMU=0
                      RETURN
               20     FMU=1/(1230.27*10**(2.7*10**7/(T+273)**2-1.84*10**4/(T+273)))
10                    RETURN
                      END

          SYMBOLIC REFERENCE MAP (R=1)

ENTRY POINTS
    4  FMU

VARIABLES      SN  TYPE            RELOCATION
   46  ERF         REAL                              44  FMU        REAL
    2  T           REAL              / /              0  TO         REAL      / /
   45  V           REAL                               1  W          REAL      / /
    0  X           REAL               F.P.

EXTERNALS          TYPE    ARGS
       MERF                  2

STATEMENT LABELS
    0  10           INACTIVE              20  20

COMMON BLOCKS     LENGTH
      / /              3

STATISTICS
  PROGRAM LENGTH                 47B       39
  CM BLANK COMMON LENGTH         3B         3
```

Handwritten annotations beside the listing:

- CALCULATES FMU - 1/DYNAMIC VISCOSITY AT A GIVEN TEMPERATURE (REQUIRED BY [illegible]) MAKING USE OF THE EMPIRICAL VISCOSITY EQUATION AND THE SOLUTION TO THE HEAT EQUATION
- "MERF" IS THE [illegible] SUBPROGRAM WHICH CALCULATES THE ERROR FUNCTION
- THIS IS THE SOLUTION TO THE HEAT EQUATION (THE + SIGN IS BECAUSE THE ERROR FUNCTION [illegible])
- SETS THE VISCOSITY [illegible] FOR TEMPERATURES BELOW 725°C. 725°C IS ARBITRARY; IT WAS FOUND THAT AT 725°C, THE VISCOSITY WAS [illegible]
- THIS IS THE EMPIRICAL VISCOSITY EQN RESULTING FROM A 2ND DEGREE POLYNOMIAL FIT [illegible] VISCOSITY VS TEMPERATURE CURVE TAKEN FROM [illegible]

FIGURE CAPTIONS

1. Martian channels Vedra Valles/Maumee Valles (top) and Maja Vallis (bottom) Vedra, Maumee and Maja Valles are interpreted to be lava erosional features. Maja Vallis also exhibits later modification by large scale flow of some substance whose nature is presently unknown.

2. One dimensional model for planar flow of a viscous substrate beneath an isothermal lava reservoir.

3. Estimate of time to erode one meter of substrate with lava as a function of lava temperature. Model 1 is due to Carr (1974). Model 2 is described in text. The third curve is the viscosity temperature relationship for a lunar basalt.

4. Volume rate of flow of substrate per unit width of a planar flow as a function of time (t) and lava temperature (T_L) The increase with time represents both a deepening of the depth of substrate that flows and an increase in velocity.

5. Estimated depth of erosion as a function of time for Model 2.

FIGURE 1

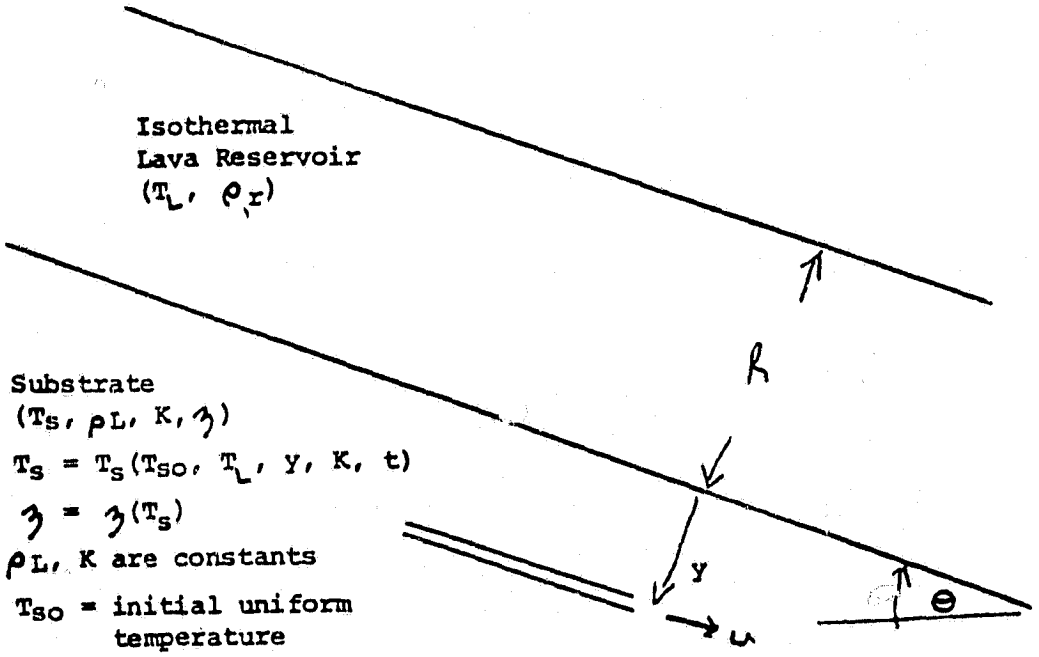
Isothermal
Lava Reservoir
(T_L, ρ_L)
R
Substrate
(T_s, ρL, K, $\mathfrak{z}$)
$T_s = T_s(T_{so}, T_L, y, K, t)$
$\mathfrak{z} = \mathfrak{z}(T_s)$
ρL, K are constants
T_{so} = initial uniform temperature
y
u
θ

FIGURE 2

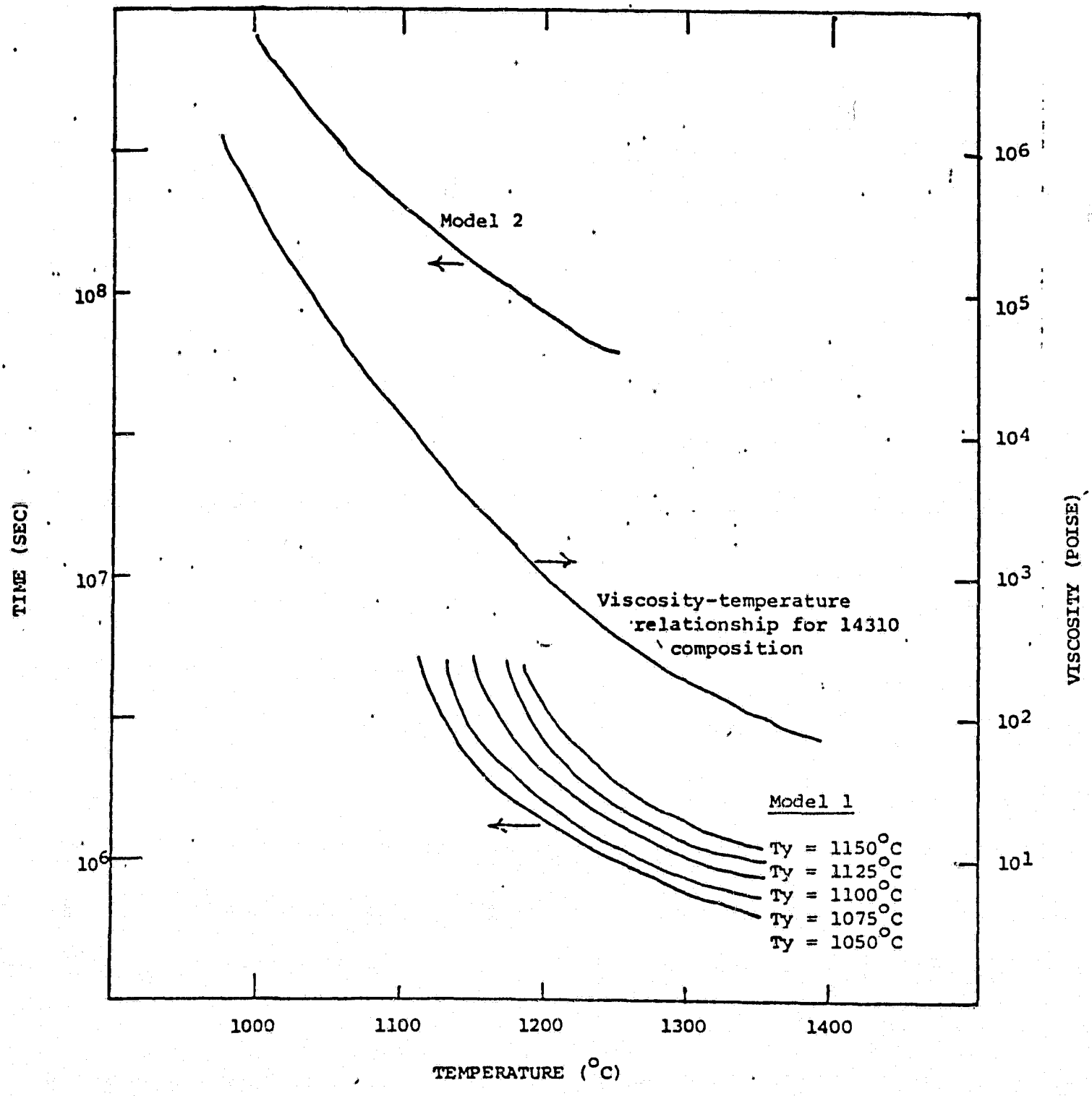
Model 2
Viscosity-temperature relationship for 14310 composition
Model 1
Ty = 1150°C
Ty = 1125°C
Ty = 1100°C
Ty = 1075°C
Ty = 1050°C
TIME (SEC)
VISCOSITY (POISE)
TEMPERATURE (°C)
10^8
10^7
10^6
10^6
10^5
10^4
10^3
10^2
10^1
1000
1100
1200
1300
1400

FIGURE 3

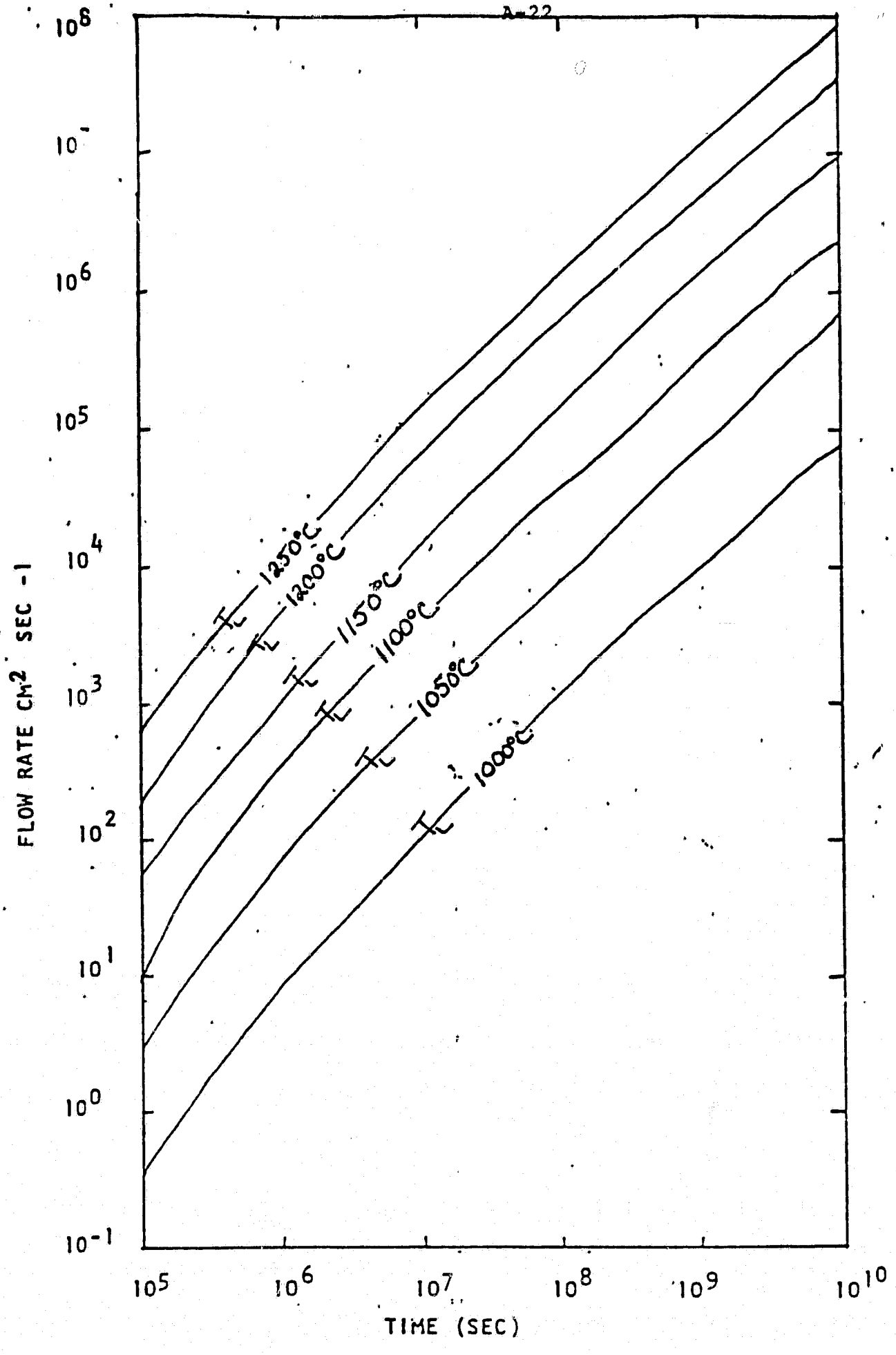
FLOW RATE CM² SEC -1
TIME (SEC)
T_L 1250°C
T_L 1200°C
T_L 1150°C
T_L 1100°C
T_L 1050°C
T_L 1000°C

FIGURE 4

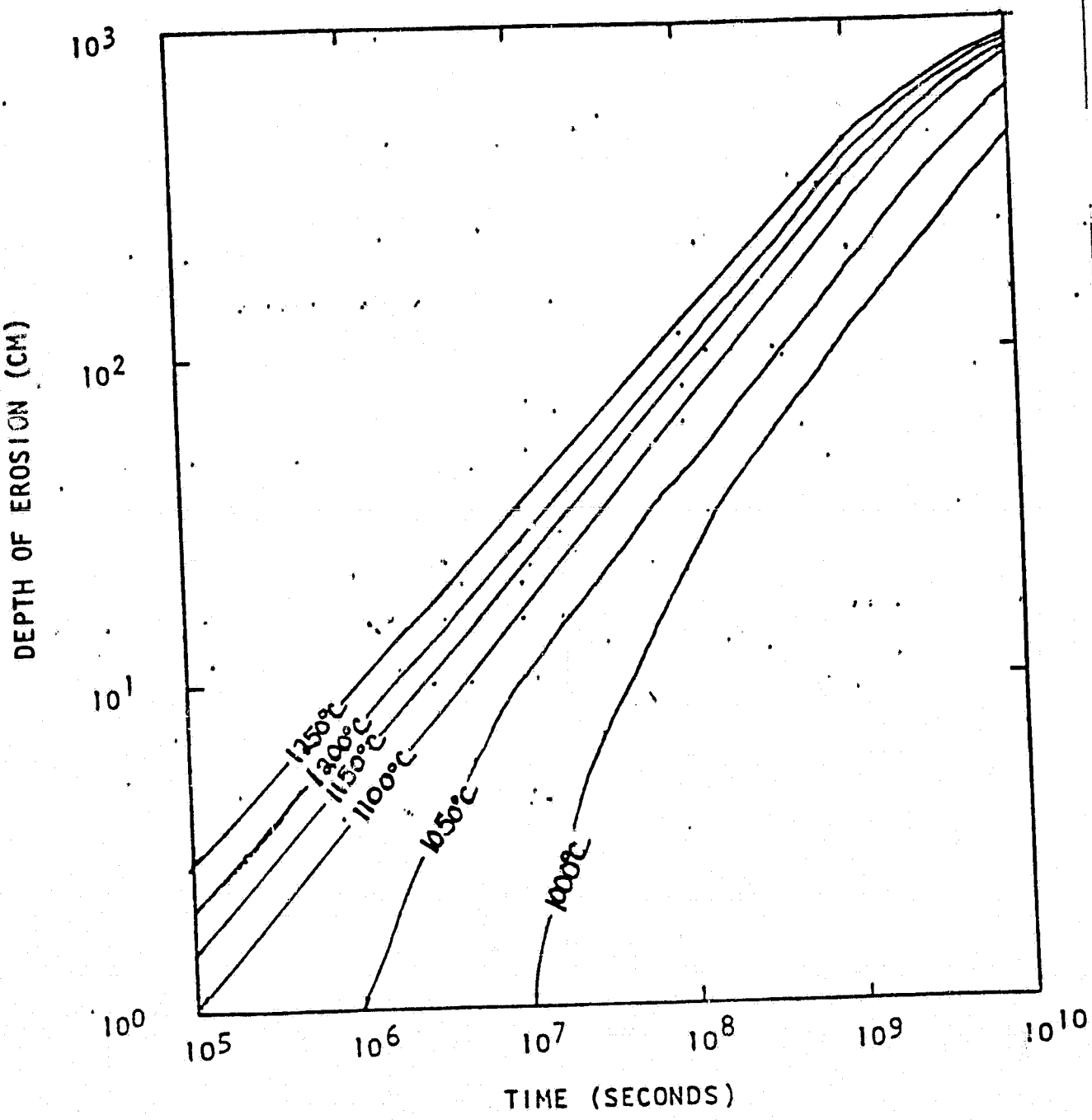

FIGURE 5

APPENDIX 3.2

TEMPERATURE DEPENDENCE OF ROCK CONDUCTIVITY

The thermal diffusion calculations presented in Appendix 3.1 do not incorporate the temperature dependence of rock conductivity. Here we describe this dependence.

THERMAL CONDUCTIVITY OF ROCKS

1. Ambient temperature values

Paper by Harai and Winkler (1974) lists the thermal diffusivity of an Apollo basalt (porosity 10%) as

7×10^{-3} cm^2/sec at 100°K

3×10^{-3} cm^2/sec at 400°K

For purpose of checking units we will assume an average of these values

$K \quad 5 \times 10^{-3}$ cm^2/sec

Thermal diffusivity may be converted to thermal conductivity using density and specific heat so that thermal cond of lunar basalt (k_{lb}) is given by:

$$k_{lb} = K \rho C \quad ; \quad \rho = 3 \text{ g cm}^{-3}$$

$$C \simeq 0.2 \text{ cal /g/}^{\circ}\text{K}$$

$$= 3 \times 10^{-3} \text{ cal cm}^{-1} \text{ sec}^{-1} {}^{\circ}\text{K}^{-1} \qquad (1)$$

This can be compared with the value for granite on PE-16 of Handbook of Physics and Chemistry which

$$k_{gr} = 1 \text{ to } 3 \quad \text{k cal m}^{-1} \text{ hr}^{-1} \text{ deg}^{-1} \qquad (2)$$

Conversion factor to units of (1) is 2.77×10^{-3}

Therefore thermal conductivity of granite is

$$K_{gr} = 3 \text{ to } 9 \times 10^{-3} \text{ cal cm}^{-1} \text{ sec}^{-1} {}^{\circ}\text{K}^{-1}$$

2. Dependence of conductivity on temperature

The conductivity of silicates shows a significant temperature dependence including cube law and inverse terms. The calculations on the next page use the relationship due to

$$k = A + B/T + CT^3$$

where $A = 0.5235 \times 10^{-3}$ cm^2/sec

$B = 0.1561$ cm^2 °K/sec

$C = 0.1367 \times 10^{-12}$ cm^2/sec °K^3

Over the temperature range 100°K to 2000°K however, the actual variation in conductivity with temeprature is not large as the B and C terms are not large.

REFERENCES

Horai and Winkler, Elastic Wave Velocities and Thermal Diffusivities of Apollo 17 Rocks, Lunar Science Conference V, p. 2895, 1974.

5th Lunar Science Conf Proceedings

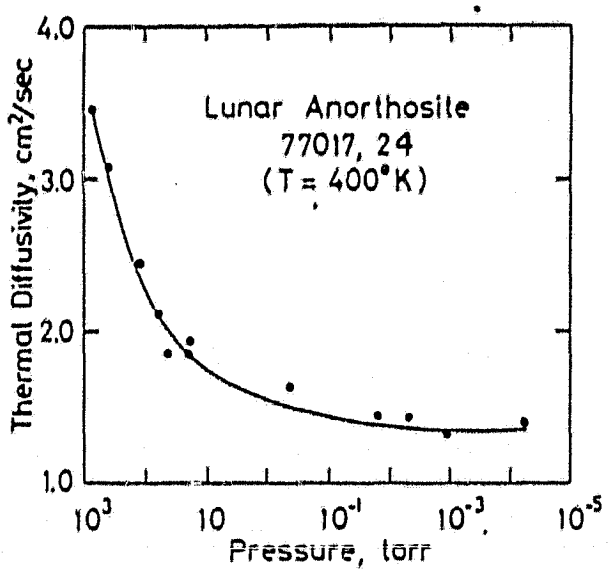

Fig. 2. Thermal diffusivity of sample 77017,24 as a function of ambient gas (air) pressure. The data are taken at temperatures around 400°K.

pressure is shown in Fig. 2. As experimentally shown by Fujii and Osako (1973) for lunar rocks and also shown by Wechsler and Glaser (1965) for particulate terrestrial rocks, the thermal diffusivity of sample 77017,24 decreases with pressure ranging 1 atm to 10^{-2} torr and stays constant at pressures below 10^{-2} torr. Similar behavior of the thermal diffusivity has been also found for sample 70215,30 by us and for Apollo 12 rock 12002,85 by Horai and Winkler (1974). These observations indicate that a vacuum of 10^{-2} to 10^{-3} torr is low enough to simulate the lunar environment, as far as the thermal diffusivity is concerned. In Fig. 3 is shown the temperature dependence of the thermal diffusivities of samples 77017,24 and 70215,30 in vacuums lower than 10^{-2} torr. The thermal diffusivities of both the samples decrease with temperature up to 400°K and stay constant or increase slightly at temperatures from 400°K to 600°K. The temperature dependence of the thermal diffusivities can be well expressed by an equation of the following type,

$$k = A + \frac{B}{T} + CT^3 \qquad (1)$$

The constants A, B, and C are obtained by least-square fit:

$$\left.\begin{aligned} A &= 0.5235 \times 10^{-3} && \text{cm}^2/\text{sec} \\ B &= 0.1561 && \text{cm}^2 \cdot {}^\circ\text{K/sec} \\ C &= 0.1367 \times 10^{-12} && \text{cm}^2/\text{sec} \cdot {}^\circ\text{K}^3 \end{aligned}\right\} \text{for } 77017,24$$

MULTIPLY by appropriate factor to OBTAIN→	$Btu_{IT}\ h^{-1}\ ft^{-1}\ F^{-1}$	Btu_{IT} in. $h^{-1}\ ft^{-2}\ F^{-1}$	$Btu_{th}\ h^{-1}\ ft^{-1}\ F^{-1}$	Btu_{th} in. $h^{-1}\ ft^{-2}\ F^{-1}$	$cal_{IT}\ s^{-1}\ cm^{-1}\ C^{-1}$	$cal_{th}\ s^{-1}\ cm^{-1}\ C^{-1}$
$Btu_{IT}\ h^{-1}\ ft^{-1}\ F^{-1}$	1	12	1.00067	12.0080	4.13379×10^{-3}	4.13656×10^{-3}
Btu_{IT} in. $h^{-1}\ ft^{-2}\ F^{-1}$	8.33333×10^{-2}	1	8.33891×10^{-2}	1.00067	3.44482×10^{-4}	3.44713×10^{-4}
$Btu_{th}\ h^{-1}\ ft^{-1}\ F^{-1}$	0.999331	11.9920	1	12	4.13102×10^{-3}	4.13379×10^{-3}
Btu_{th} in. $h^{-1}\ ft^{-2}\ F^{-1}$	8.32776×10^{-2}	0.999331	8.33333×10^{-2}	1	3.44252×10^{-4}	3.44482×10^{-4}
$cal_{IT}\ s^{-1}\ cm^{-1}\ C^{-1}$	2.41909×10^{2}	2.90291×10^{3}	2.42071×10^{2}	2.90485×10^{3}	1	1.00067
$cal_{th}\ s^{-1}\ cm^{-1}\ C^{-1}$	2.41747×10^{2}	2.90096×10^{3}	2.41909×10^{2}	2.90291×10^{3}	0.999331	1
$kcal_{th}\ h^{-1}\ m^{-1}\ C^{-1}$	0.671520	8.05824	0.671969	8.06363	2.77592×10^{-3}	2.77778×10^{-3}
$J\ s^{-1}\ cm^{-1}\ K^{-1}$	57.7789	6.93347×10^{2}	57.8176	6.93811×10^{2}	0.238846	0.239006
$W\ cm^{-1}\ K^{-1}$	57.7789	6.93347×10^{2}	57.8176	6.93811×10^{2}	0.238846	0.239006
$W\ m^{-1}\ K^{-1}$	0.577789	6.93347	0.578176	6.93811	2.38846×10^{-3}	2.39006×10^{-3}
$mW\ cm^{-1}\ K^{-1}$	5.77789×10^{-2}	0.693347	5.78176×10^{-2}	0.693811	2.38846×10^{-4}	2.39006×10^{-4}

MULTIPLY by appropriate factor to OBTAIN→	$kcal_{th}\ h^{-1}\ m^{-1}\ C^{-1}$	$J\ s^{-1}\ cm^{-1}\ K^{-1}$	$W\ cm^{-1}\ K^{-1}$	$W\ m^{-1}\ K^{-1}$	$mW\ cm^{-1}\ K^{-1}$
$Btu_{IT}\ h^{-1}\ ft^{-1}\ F^{-1}$	1.48916	1.73073×10^{-2}	1.73073×10^{-2}	1.73073	17.3073
Btu_{IT} in. $h^{-1}\ ft^{-2}\ F^{-1}$	0.124097	1.44228×10^{-3}	1.44228×10^{-3}	0.144228	1.44228
$Btu_{th}\ h^{-1}\ ft^{-1}\ F^{-1}$	1.48816	1.72958×10^{-2}	1.72958×10^{-2}	1.72958	17.2958
Btu_{th} in. $h^{-1}\ ft^{-2}\ F^{-1}$	0.124014	1.44131×10^{-3}	1.44131×10^{-3}	0.144131	1.44131
$cal_{IT}\ s^{-1}\ cm^{-1}\ C^{-1}$	3.60241×10^{2}	4.1868	4.1868	4.1868×10^{2}	4.1868×10^{-3}
$cal_{th}\ s^{-1}\ cm^{-1}\ C^{-1}$	3.6×10^{2}	4.184	4.184	4.184×10^{2}	4.184×10^{-3}
$kcal_{th}\ h^{-1}\ m^{-1}\ C^{-1}$	1	1.16222×10^{-2}	1.16222×10^{-2}	1.16222	11.6222
$J\ s^{-1}\ cm^{-1}\ K^{-1}$	86.0421	1	1	1×10^{2}	1×10^{3}
$W\ cm^{-1}\ K^{-1}$	86.0421	1	1	1×10^{2}	1×10^{3}
$W\ m^{-1}\ K^{-1}$	0.860421	1×10^{-2}	1×10^{-2}	1	10
$mW\ cm^{-1}\ K^{-1}$	8.60421×10^{-3}	1×10^{-3}	1×10^{-3}	0.1	1

CALCULATIONS OF THERMAL DIFFUSIVITY AS A FUNCTION OF TEMPERATURE IN LUNAR BASALT IN RANGE 100°K + 2000°K +

HP 97 Program

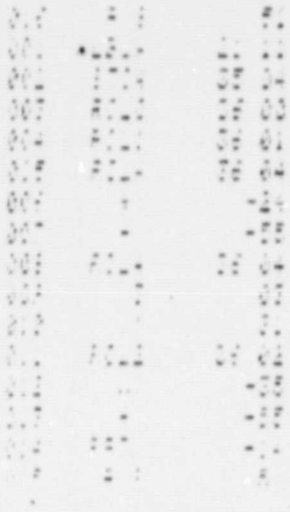

Temp	Thermal Diffusivity cm^2/sec
100°K	
1050°K	
1100°K	
2000°K	

$$k = A + B/_T + CT^3 \qquad (1)$$

A = 0.5235×10^{-3} cm^2/sec Register 0

B = 0.1561 $cm^2\ ^\circ K/sec$ Register 1

C = 0.1367×10^{-12} $cm^2/sec\ ^\circ K^3$ Register 2

Method: Enter temperature and key A and program prints the diffusivity using equation (1)

APPENDIX 3.3

HAND CALCULATOR PROGRAM TO DETERMINE TEMPERATURE FIELD IN A LAMINAR FLOW OF CONSTANT VISCOSITY WITH UNIFORM HEAT INPUT AT THE BASE OF THE FLOW

C-2

APPENDIX 5.2

Program Description

Program Title VT FIELD FOR STEADY FULLY DEVELOPED FLOW.

Name **Date**

Address

City **State** **Zip Code**

Program Description, Equations, Variables, etc.

This program computes the velocity and temperature field for a steady, fully developed flow down an inclined plane, assuming laminar flow. It also prints the Reynolds number so that the validity of the laminar flow model can be assessed. The boundary condition on the velocity field are no slip at the base of the flow. The boundary conditions on the temperature field are a constant heat influx through the base of the flow and no heat efflux from the top of the flow implying that all heat is absorbed downstream.

The flow velocity (u) is given by:

$$u = \frac{\rho g \sin\phi}{2\nu}(y_0^2 - y^2) \qquad \text{where } \rho = \text{density}, g = \text{grav. acc.}$$

$$= C_1(y_0^2 - y^2) \qquad \phi = \text{slope}, \nu = \text{viscosity}$$

y = depth coordinate, y_0 = total depth.

Local Reynolds No. $R_L = \frac{u_s(y_0 - y)}{\nu}$ $\qquad y_0 - y$ = depth to bottom.

$$C_2 = \frac{\alpha}{5k y_0^3}; \quad T = C_2[5y_0^4 - 6y_0^2 y^2 + y^4 - 12y_0^4] \qquad x = \text{location along flow}$$

$$\frac{\partial T}{\partial y} = \frac{\alpha}{5k y_0^3}[-12y_0^2 y + 4y^3] \qquad k = \text{conductivity}$$

α = heat flow

Operating Limits and Warnings

DO NOT USE THIS SPACE

STEP	KEY ENTRY	KEY CODE	COMMENTS	STEP	KEY ENTRY	KEY CODE	COMMENTS
			Calculate C1				
			Print C1				
			Print C2				
			Calculate w & Pw				
			Print U				
			Print Pw				

100	
110	

REGISTERS

0	1	2	3	4	5	6	7	8	9
S0	S1	S2	S3	S4	S5	S6	S7	S8	S9

A	B	C	D	E	I

User Instructions

VT - FIELD.

STEP	INSTRUCTIONS	INPUT DATA/UNITS	KEYS	OUTPUT DATA/UNITS
1	Load parameters of Flow			
	Thermal diffusivity (α)	cm^2/sec	STO 0	
	Downstream distance (x)	cm	STO 1	
	Stream depth (y_0)	cm	STO 2	
	Heat in Flux (q_0)	$cal/cm^2/sec$	STO 3	
	Thermal conductivity (k)	$cal/cm/sec/°K$	STO 4	
	Slope angle (ϕ)	degrees	STO 5	
	Gravitational accel. (g)	cm/sec^2	STO 6	
	Dynamic viscosity (μ)	poise	STO 7	
	Density of Fluid (ρ)	gm/cm^3	STO 9	
2	Calculate constant parameters which are output on printer.		A	C_1
				C_2
3	Calculate velocity and local Reynolds number at depth y_2	y_2 (cm)		
			E	U (cm/sec)
				R_L
4.	Calculate temperature at depth y_2	y_2 (cm)		
			C	T (°K)
5	Calculate temperature gradient at depth y_2			
		y_2 (cm)		
			D	$\frac{\partial T}{\partial y}\Big\|_{y_2}$ (°K/cm)

APPENDIX 3.4

APPENDIX 3.4

Comparison of conditions for laminar and turbulent flow in several fluids of geological interests

Basic Physical Parameters

Viscosity coefficient

air = 0.14 cgs units

= 140 g/(cm)(sec)

poise = cgs unit of absolute viscosity = g /sec x c

Poise = cgs unit of abs. visc. = gm/sec x cm

Stoke = cgs unit of kin. visc. = g /sec x cm x dens (^{o}F)

Viscosity of water at 20^{o}C = 0.01 poise

$$v = \frac{\pi p r^4}{8 \ell \eta}$$ Flow of liquid through a tube

If the tangential force exerted by a layer of fluid upon one adjacent layer is one dyne for a space rate of variation of tangential velocity then viscosity is one poise

$$= \frac{\text{dyne}}{\text{cm}^2} \cdot \left(\frac{\text{cm}}{\text{sec}} \cdot \frac{1}{\text{cm}}\right)^{-1} = \frac{\text{dyne-seconds}}{\text{cm}^2} = \frac{\text{gm}}{\text{sec}^2} \cdot \frac{\text{cm}}{\text{cm}^2} \cdot \frac{\text{sec}}{\text{cm}^2} = \frac{\text{gm}}{\text{cm sec}}$$

Air = 182×10^{-6} poise at 18^{o}C [1]

Water = 1.002×10^{-2} poise at 20^{o}C

Lava = 6.5 to 7.5×10^{3} poise at 1130 to 1135^{o}C

---

[1] P F.56 Handbood of Chemistry and Physics

[2] P F.49 Handbook of Chemistry and Physics

[3] Moore, H.J. and Schaber, G.C. (1975), An Estimate of the Yield Strength of the Imbrium Flows. Proc. Lun. Sci. Conf. 6th, p. 101-118. (P. 105 quoting work by Shreve et al., 1968).

APPENDIX 3.4

Comparison of conditions for laminar and turbulent flow in several fluids of geological interests

Basic Physical Parameters

Viscosity coefficient

air = 0.14 cgs units

= 140 g/(cm) (sec)

poise = cgs unit of absolute viscosity = g /sec x

Poise = cgs unit of abs. visc. = gm/sec x cm

Stoke = cgs unit of kin. visc. = g /sec x cm x dens (^{o}F)

Viscosity of water at 20^{o}C = 0.01 poise

$$v = \frac{\pi p r^4}{8 t \eta}$$ Flow of liquid through a tube

If the tangential force exerted by a layer of fluid upon one adjacent layer is one dyne for a space rate of variation of tangential velocity then viscosity is one poise

$$= \frac{\text{dyne}}{\text{cm}^2} \cdot \left(\frac{\text{cm}}{\text{sec}} \cdot \frac{1}{\text{cm}}\right)^{-1} = \frac{\text{dyne-seconds}}{\text{cm}^2} = \frac{\text{gm cm}}{\text{sec}^2} \cdot \frac{\text{sec}}{\text{cm}^2} = \frac{\text{gm}}{\text{cm sec}}$$

Air = 182×10^{-6} poise at 18^{o}C [1]

Water = 1.002×10^{-2} poise at 20^{o}C

Lava = 6.5 to 7.5×10^{3} poise at 1130 to 1135^{o}C

---

[1] P F.56 Handbood of Chemistry and Physics

[2] P F.49 Handbook of Chemistry and Physics

[3] Moore, H.J. and Schaber, G.C. (1975), An Estimate of the Yield Strength of the Imbrium Flows. Proc. Lun. Sci. Conf. 6th, p. 101-118. (P. 105 quoting work by Shreve et al., 1968).

R (Reynolds number) $= \rho \frac{VL}{\eta}$

Flow is laminar generally for $R < 1000$

Flow is turbulent generally for $R > 1000$

Substance	g/cm^3	Poise	$(stoke^{-1})$	L cm	V cm/sec	R
Air (earth)	1.205×10^{3} [1]	1.82×10^{-6}	6.59	10^2 10	10 10	6590 659
Water	1.0	1.002×10^{2}	100	10 100	1 10	1000 10^5
Lava	3.0	1×10^{3}	3×10^{-3}	10^3	3×10^2	900
Air (Mars)	1×10^{-5}	160×10^{-6}	6.2×10^{-2}	10^3	3×10^2	1.8×10^4

---

[1] Handbook of Chem. Phys. P F-11

[2] Carr, M.H., The Role of Lava Erosion in the Formation of Lunar Rilles and Martian Channels, Icarus, 22, 1-23, 1973.

[3] Viscosity is indep of pressure but does depend on temp ($\alpha T^{\frac{1}{2}}$). Assume 230°K in atmosphere on Mars. Yovorsky and Detlaf (see Handbook of Physics, Mir Publishers, Moscow).

The conclusion from this comparison is that water and air flow will be turbulent in all conditions of the scale of those likely to be found in nature whereas there is a regime of relatively small scale or low velocity flow or both where lava will flow in a laminar fashion. Because of the lower density of the atmosphere on Mars, it is much closer to being in a laminar regime than on the earth - the atmsopheric viscosity is about the same. However, it still isn't in the same ball park. Interestingly, the kinematic viscosity is approaching that of lava.

APPENDIX 3.5

COMPUTER PROGRAM FOR COMPUTING EQUILIBRIUM SLOPE PROFILE FOR SIMPLE PHENOMENOLOGICAL MODELS OF LAVA EROSION

This is a program for a Hewlett Packard 97 programmable calculator that determines the slope profile for a slope that has reached an equilibrium shape under the action of thermo-mechanical erosion.

EVALUATION OF $K = \int_0^H \frac{(1 - F^2(H))^{\frac{1}{2}}}{F(H)}$

FOR $F(H) = (P_o\, e^{H/Ho})^{1/m-1}$*

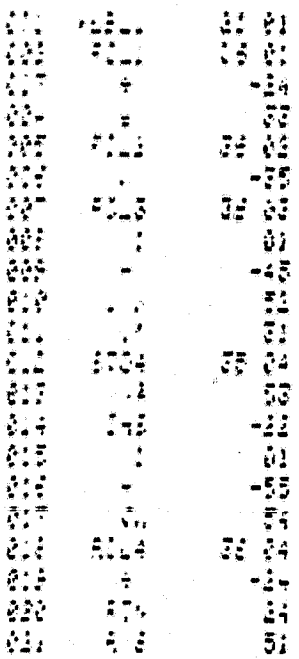

REG	
1	Ho
2	Po
3	m
4	F(H)

* This program segment can be used in conjunction with the HP-97 Numerical Integration (Simpson's Rule) program to evaluate the given integral in terms in Po, Ho, m and H. A future program should be structured to first calculate Po and Ho from equation (18) and (19) and store them as constants for use in the integration procedure rather than repetitively recalculating them.

APPENDICES TO TASK 4

4.1 Abstract of Hodgson (1969) work on lava flow similitude using carbowaxes with data on physical properties of carbowax and lava flows and model parameters for lava

4.2 Computer simulation test programs

APPENDIX 4.1

ABSTRACT OF HODGSON (1969) WORK ON LAVA FLOW SIMILITUDE USING CARBOWAXES WITH DATA ON PHYSICAL PROPERTIES OF CARBOWAX AND LAVA FLOWS AND MODEL PARAMETER VALUES FOR WAX AND LAVA

ABSTRACT

The mechanism of emplacement of viscous flows was investigated experimentally with Carbowax materials. The design requirements for modeling the emplacement of natural lava flows of high and low SiO_2 content were considered. These requirements were found to be very complex and the laboratory wax models contained distortions. However, Carbowax flows are affected by similar heat and mass transfer processes as natural flows and behave in similar ways. Hence, they provide a qualitative and possibly semi-quantitative insight into the development of natural lava flows.

The models of emplacement and many structural features observed in the experimental flows are similar to those in nature. The influeence of volume, slope, initial velocity, and extrusion rate on the Carbowax flows was investigated. The following scaling relationship was developed for maximum flow length relative to any reference flow as a function of the physical parameters investigated.

$$\frac{L}{L_o} = \left(\frac{V}{V_o}\right)^a \left(\frac{S}{S_o}\right)^b \left(\frac{\mu}{\mu_o}\right)^c \left(\frac{\dot{M}}{\dot{M}_o}\right)^d$$

$a = 0.382 \pm .136$

$b = 0.419 \pm .085$

$c = -1.81 \pm .72$

$d = 0.469 \pm .014,$
$-0.174 \pm .089$

The positive value of d would apply to extrusion rates in nature of less than 430 million m^3/day. The negative value applies to higher extrusion rates.

APPENDIX ≠ (cont'd.)

(From widdicombe and McGetchin, 1976)

Model Parameter Values for Lava and Carbowax Flows

Pi Terms		Basic Lava Flows	Acidic Lava Flows	Carbowax 4000 Flows	Carbowax 20M Flows
Width Ratio	$\frac{b}{\ell}$	.20	.20	.20	.20
Depth Ratio	$\frac{d}{\ell}$	.02	.10	.06	.20
Roughness	r	variable	variable	smooth	smooth
Froude Number	$\frac{v^2}{gd}$	10^{-3}	10^{-6}	10^{-3}	10^{-5}
Reynolds Number	$\frac{\rho v d}{\mu}$	10^{-1}	10^{-6}	10^{-4}	10^{-6}
Weber Number	$\frac{\rho v^2 d}{\sigma}$	10^{2}	10^{1}	10^{-4}	10^{-6}
Nusselt Number	$\frac{h_c \ell}{k}$	$1(10^7)h_c$	$1(10^7)h_c$	$6(10^3)h_c$	$6(10^3)h_c$
Prandtl Number	$\frac{\mu C_p}{k}$	10^{7}	10^{11}	10^{5}	10^{6}
Eckert Number	$\frac{v^2}{C_p T}$	10^{-8}	10^{-10}	10^{-9}	10^{-11}

APPENDIX 4.2
FINITE ELEMENT MODELLING EXERCISES

During the time period from Aug. to Nov. 1979, several programs were written and experimented with to develop an understanding of two dimensional finite element models. They fall into two categories: those related to the vorticity transport equation $\frac{D\bar{\zeta}}{D\bar{t}} = \bar{\nu}\,\bar{\Delta}^2\,\bar{\zeta}$, and those which solve the Poisson equation $\nabla^2\bar{\psi} = \bar{\zeta}$. The overbars represent dimensional quantities. A complete solution to the flow problem involves successively solving each of the two equations for each time step.

A basic finite difference form of the vorticity transport equation is (see Roche, Equation 3.165):

$$\frac{\zeta_i^{n+1} - \zeta_i^{n-1}}{2\Delta t} = -u\,\frac{(\zeta_{i+1}^n - \zeta_{i-1}^n)}{2\Delta x} + \alpha\,\frac{(\zeta_{i+1}^n + \zeta_{i-1}^n - 2\zeta_i^n)}{(\Delta x)^2} \qquad 4.2.1$$

ADVECTION TERM DIFFUSION TERM

where u = velocity

α = diffusion constant

superscripts refer to the time step

subscripts refer to the cell number

this is a centered time, centered space (Ctcs) equation, since the average in the 'time' term (LHS) is centered at the present step, and the average in the two 'space' terms (RHS) is centered at the cell whose new value is being computed.

This method is unconditionally unstable (Roche, p. 36). However, if only the advection term is considered, the method yields stable solutions. To get back the diffusion term, the method of Du Fort and Fankl was used. In this method, the diffusion term is replaced with the expression

$$\alpha \frac{\zeta_{i+1}^{n} + \zeta_{i-1}^{n} - \left(\zeta_i^{n+1} + \zeta_i^{n-1}\right)}{(\Delta x)^2} \qquad 4.2.2$$

The only difference is in the last term in the numerator, which becomes the sum of past and future values at the cell in question.

This is the Du-Fort Frankl leapfrog method, and the programs employing it are DFFLF (the one dimensional case) and 2DFFLF (the two dimensional case). The programs as written contain the boundary and initial conditions, and also contain the condition u = 0. Thus they, at present, deal only with diffusion. In fact, the 2D program does not contain the advection term at all. The programs were tested (and compared with analytic solutions graphed by the programs ANATST and BNATST) with two sets of initial conditions: $\zeta = 100$, and $\zeta = 100 \sin \frac{\pi x}{\text{length}}$.

The Du-Fort Frankl leapfrog method is not transportive and introduces phase errors when u = 0, so in the next exercise, the Du-Fort Frankl programs were modified to incorporate second upwind differencing in the advection terms. This is essentially a forward space method, where the direction is decided by the sign of u. The equation (for advection only) is:

$$\frac{\zeta_i^{n+1} - \zeta_i^{n}}{\Delta t} = - \frac{v_+ \zeta_+ - v_- \zeta_-}{\Delta x} \qquad 4.2.3$$

where v_+ is the average of the velocity at cell i and cell i + 1

v_- is the average of the velocity at i and cell i + 1

ζ_+ is the average of ζ_i^n and ζ_{i+1}^n

ζ_- is the average of ζ_i^n and ζ_{i-1}^n

Note that this method is a forward time method. This makes it incompatible with the Du-Fort Frankel. Nonetheless, hybrid programs were written by replacing the advection term of equation 4.2.1 with the RHS of equation 4.2.3. These programs are called SUDLF and 2SUDLF. One of the problems with these programs is that the advection term updates itself only every other iteration, due to the leapfrogging inherent in Du-Fort Frankel, and effectively proceeds at half speed, while the diffusion term proceeds at full speed.

The other programs solve the Poisson equation and use the method of successive over relaxation. This is an iterative method which converges asymmetrically on the solution. The finite difference equation is:

$$\psi_{ij}^{k+1} = \psi_{ij}^{k} + \frac{\omega}{2(1+\beta^2)} \qquad 4.2.4$$

$$\left[\psi_{i+1,j}^{k} + \psi_{i-1,j}^{k+1} + \beta^2(\psi_{i,j+1}^{k} + \psi_{i,j-1}^{k+1}) - \Delta x^2 \zeta_{ij} - 2(1+\beta^2)\psi_{ij}^{k}\right]$$

where $\beta \frac{\Delta x}{\Delta y}$ = cell size aspect ratio

ω = relaxation parameter $1 \leq \omega < 2$

ω controls the speed of convergence, and the optimum ω to use depends on the geometry and boundary conditions of the problem, and can be found analytically only in a limited number of cases. For the rest of the cases, the optimum ω must be found by trial and error.

Two programs were rewritten that solve Poisson's equation with Dirichlet conditions. They are SOR and SORNQ3. The difference between them is the boundary conditions. SOR has a source in the center, and has the outside held at zero potential, while SORNQ3 has no sources, and has two facing boundaries at a potential of 100, and the other two boundaries held at zero. The output of these two programs was compaired to the analytic solution as plotted by SORTST and SOR2T respectively.

A third version of the program, NEUSOR, solves Poissons equation with mixed boundary conditions and no sources. The boundary conditions are Neuman on two facing edges, and Dirichlet on the other two facing edges.

A program for finding the optimum ω for the NEVSOR program was also written. It employs a decimal search, and counts the number of iterations required for convergence of a particular problem at each ω. A binary search was not employed because if it were, the program would spend a large part of it's time in overrun conditions.

Experience gained in exercising these programs was used in re-formulating the lava erosion problem, and writing the programs needed to solve it.

LIST OF PROGRAMS

DFFLF	solves 1-D vorticity transport equation using Du-Fort Frankel leapfrog method.
SUDLF	solves 1-D vorticity transport equation using Second Upwind Differencing on the advection term, and the Du-Fort.
ANATST	graphs analytic solution of heat flow equation with IC's $T = \sin \frac{\pi x}{\text{length}}$
BNATST	graphs analytic solution of heat flow equation with IC's T = 100, except T = 0 at boundarys.
2DFFLF	solves 2-D vorticity equation using Du-Fort Frankel leapfrog method, but with no advection term in equation.
2SUDLF	solves 2-D vorticity transport equation using second upwind differencing on the advection term, and the Du-Fort Frankel method on the diffusion term.
SOR	solves Poisson's equation with boundaries held at zero potential and a source in the center, using the Successive Over-relaxation.
SORNQ3	
SORTST	graphs analytic solution of the problem solved by SOR.
SOR2T	graphs analytic solution of the problem solved by SORNQ3.
NEUSOR	solves Posson's equation using Successive Over-relaxation for mixed Dirchlet and Neumann B.C.'s, and no sources.
NWSOR	Finds optimum ω to use for NEUSOR.

APPENDIX 4.3. FORTRAN Program for two dimensional model of thermal erosion for a plane laminar constant viscosity flow with a yield temperature.

```
                FUNCTIONS INLINE ARE:    ALL

ISN 0002              INTEGER PP,DD,PRINT,PT,    FLOOR,O,AAA,FLIP,      HCS
ISN 0003              REAL MIX,MELTEM,LENGTH,KAPPA
                C      ALL OTHER VARIABLES FOLLOW IJKLMN CONVENTION
ISN 0004              DIMENSION T(12,17,2),PT(12,17),OPT(17,12),F(12,17),V(17),DY(17
                     1,Y(17)
ISN 0005              ID=5
ISN 0006              AAA=6
ISN 0007              THR=1200.
ISN 0008              MIX=0.1E-04
ISN 0009              ANG=30.
ISN 0010              TH=(ANG/180.)*3.141592654
ISN 0011              PP=30
ISN 0012              TMAX=96.
ISN 0013              ROC=0.25
ISN 0014              VMAX=1000.
ISN 0015              DT=400.
ISN 0016              JM=17
ISN 0017              JMM1=JM-1
ISN 0018              JMM2=JM-2
ISN 0019              JMM3=JM-3
ISN 0020              AL=1.356E-12
ISN 0021              PRINT=-1
ISN 0022              ITER=-1
ISN 0023              TIME=-1.*DT
ISN 0024              MELTEM=1300.
ISN 0025              AMBTEM=20.
ISN 0026              FLOOR=11
ISN 0027              IFLP1=FLOOR+1
ISN 0028              G=980.
ISN 0029              H=150.
ISN 0030              LENGTH=0.1E 08
ISN 0031              O=1
ISN 0032              N=2
ISN 0033              DX=LENGTH/10.
ISN 0034              KAPPA=0.04
ISN 0035              WRITE(AAA,250)   KAPPA,ROC,G,ANG,H,VMAX,MIX
ISN 0036     250      FORMAT(//40X,6HKAPPA=    ,F13.5/40X,6HROC=     ,F13.5/
                     1   40X,6HG=       ,F13.5/40X,6HANG=     ,F13.5/40X,
                     2   6HH       ,F13.5/40X,6HVMAX=    ,F13.5/40X,
                     3   6HMIX=    ,F13.5//)
ISN 0037              DO 1 I=1,12
ISN 0038              DO 2 J=1,FLOOR
ISN 0039              T(I,J,O)=AMBTEM
ISN 0040     2        CONTINUE
ISN 0041              DO 3   J=IFLP1,JM
ISN 0042              T(I,J,O)=MELTEM
ISN 0043     3        CONTINUE
ISN 0044     1        CONTINUE
ISN 0045              READ(2,101)   (DY(J),J=2,JMM1)
ISN 0046     101      FORMAT (15F4.1)
```

```
ISN 0047              DO 1050   J=2,JMM1
ISN 0048       1050 DY(J)=150.*DY(J)
ISN 0049              Y(JM-1)=DY(JM-1)/2.
ISN 0050              DO 51    JJ=2,JMM2
ISN 0051              J=JM-JJ
ISN 0052        51     Y(J)=Y(J+1)+DY(J+1)/2.+DY(J)/2.
ISN 0053              DO 56    J=2,JMM1
ISN 0054              IF (Y(J)-H) 57,58,58
ISN 0055        58    V(J)=0
ISN 0056              GOTO 56
ISN 0057        57    V(J)=VMAX*(1.-(Y(J)/H)**2)
ISN 0058        56    CONTINUE
ISN 0059        430    ITER=ITER+1
ISN 0060              TIME=TIME+DT
ISN 0061              DO 5 J=2,FLOOR
ISN 0062              T(1,J,0)=T(2,J,0)
ISN 0063              T(12,J,0)=T(11,J,0)
ISN 0064        5     CONTINUE
ISN 0065              DO 6    J=IFLP1,JMM1
ISN 0066                T(1,J,0)=MELTEM
ISN 0067              T(12,J,0)=T(11,J,0)
ISN 0068        6     CONTINUE
ISN 0069              DO 11 I=1,12
ISN 0070              DO 12 J=1,JM
ISN 0071              F(I,J)=0
ISN 0072        12    CONTINUE
ISN 0073        11    CONTINUE
ISN 0074              DO 7 I=2,11
ISN 0075              T(I,1,0)=T(I,2,0)
ISN 0076              T(I,JM,0)=T(I,JM-1,0)
ISN 0077          333 DO 8    J=2,JMM1
ISN 0078              DYU=DY(J+1)
ISN 0079              DYC=DY(J)
ISN 0080              DYD=DY(J-1)
ISN 0081              VEL=V(J)
ISN 0082              GOTO 650
ISN 0083         2004 IF (T(I,J,0) .LT. THR) VEL=0
ISN 0085              IF ((T(I,J,0) .GT.THR) .AND.(J .LE. FLOOR)) GOTO 620
ISN 0087        620   FTT=MIX*(T(I,J+1,0)-T(I,J,0))
ISN 0088              F(I,J)=FTT+F(I,J)
ISN 0089              F(I,J+1)=-FTT+F(I,J+1)
ISN 0090        650   ONE=VEL*(T(I-1,J,0)-T(I,J,0))/DX
ISN 0091              GO TO 660
ISN 0092         2005 IF ((T(I,J,0) .GE. THR) .OR. (T(I-1,J,0) .LT.THR)) GOTO 660
ISN 0094              F(I-1,J+1)=ONE+F(I-1,J+1)
ISN 0095              ONE=0
ISN 0096        660   TWO=KAPPA*(T(I-1,J,0)+T(I+1,J,0)-2.*T(I,J,0))/DX**2
ISN 0097              THREEU=(T(I,J+1,0)-T(I,J,0))/((DYU+DYC)/2.)**2
ISN 0098              THREED=(T(I,J-1,0)-T(I,J,0))/((DYD+DYC)/2.)**2
ISN 0099              THREE=KAPPA*(THREEU+THREED)
ISN 0100              T(I,J,N)=T(I,J,0)+(ONE+TWO+THREE+F(I,J))*DT
ISN 0101              IF((J .NE. JM-1) .AND. (J .NE. 2))GOTO 720
ISN 0103              RAD=T(I,J,N)-AL*((T(I,J,N)+273.)**4-(AMBTEM+273.)**4)/(DYC*RO(
ISN 0104              IF ((J.EQ.JM-1).OR.(J.EQ.2)) T(I,J,N)=RAD
ISN 0106        720   JJJ=13-J
ISN 0107        8     CONTINUE
ISN 0108        7     CONTINUE
ISN 0109              FLM3=FLOOR-3
```

```
ISN 0110              TRGR=T(11,FLM3,N)
ISN 0111              DO 9 I=1,12
ISN 0112              DO 10 J=1,JM
ISN 0113              JJJ=JM+1-J
ISN 0114              OPT(JJJ,I)=     T(I,J,0)
ISN 0115        10    CONTINUE
ISN 0116        9     CONTINUE
ISN 0117              IF (MOD(ITER,PP))970,2001,970
ISN 0118        2001   CONTINUE
ISN 0119              TIMM=TIME/3600.
ISN 0120              WRITE (AAA,22)ITER,TIMM
ISN 0121           22 FORMAT(1X,11HITERATION# ,I8,12X,F5.1,6H HOURS/)
ISN 0122              WRITE (AAA,920) ((OPT(I,J),J=1,12),I=1,JM)
ISN 0123           920 FORMAT(12(1X,F7.2))
ISN 0124              WRITE (AAA,935)
ISN 0125        935   FORMAT(//)
ISN 0126           970 IF(TRGR.LE.THR)   GO TO 177
ISN 0128              WRITE(AAA,2025)
ISN 0129           2025 FORMAT(1X,3HEND)
ISN 0130              GO TO 666
ISN 0131           2006 DO 200    I=1,12
ISN 0132              DO 176    JJ=1,JMM3
ISN 0133              J=JM-JJ
ISN 0134              T(I,J,N)=((DY(J)-0.2)*T(I,J,N)+0.2*T(I,J-1,N))/DY(J)
ISN 0135        176   CONTINUE
ISN 0136              T(I,2,N)=((DY(2)-0.2)*T(I,2,N)+0.2*AMBTEM)/DY(2)
ISN 0137           200 CONTINUE
ISN 0138              ITTP1=ITER+1
ISN 0139              TPDT=(TIME+DT)/60.
ISN 0140              WRITE(AAA,178)   ITTP1,TPDT
ISN 0141           178 FORMAT(//2X,27HREZONED AT ITERATION NUMBER,2X,I8,12X,F13.5,2X,
                     1   3HMIN)
ISN 0142        177   CONTINUE
ISN 0143        93    CONTINUE
ISN 0144              FLIP=O
ISN 0145              O=N
ISN 0146              N=FLIP
ISN 0147              IF (TIMM .GT. TMAX)  GOTO 666
ISN 0149              GOTO 430
ISN 0150        666   STOP
ISN 0151              END
```

APPENDIX 4.4

Abstract of Proposal
Submitted in July 1979
for Further Investigations of
Lava Erosion

PROPOSAL SUMMARY

PRINCIPAL INVESTIGATOR:
(Name, address, tel.no.)

James A. Cutts
Planetary Science Inst/Science Applicatio Inc.
283 S. Lake Ave. Suite 218
Pasadena, CA 91101

CO-INVESTIGATORS:
(Name only)

Karl R. Blasius
Clark R. Chapman
Wm. James Roberts

Title: Geophysical Constraints on Lunar & Planetary Volcanism

ABSTRACT (Single-spaced, type within box below. Include: a. Brief statement of the overall objectives and justification of the work; b. Brief statement of the accomplishments of the prior year, or "new proposal"; c. Brief listing of what will be done this year as well as how and why; and d. One or two of your recent publications relevant to the proposed work.):

a) We propose a one-year follow on to our investigations of the role of volcanism in forming features of planetary surfaces. Its goals are to refine and extend the qualitative and quantitative understanding of the formation of volcanic features. Task 1 is a continuation of the study of the physical mechanism of thermal lava erosion with application to the origins of some lunar sinuous rilles and martian channels. Task 2 is a continuation of an investigation of the origin of small lunar craters and its implications for mare basalt petrogenesis.

b) Through March 1979 we performed a classification of small crater features, catalogued central volcanic constructs, and gathered basic physical data on martian central volcanic constructs.

c) In Task 1, physical modeling studies will be used to test the validity of thermal erosion codes. A solid-liquid wax system will be used. Initial phenomenological investigations of flow responses to obstacles, channel sinuosity, and variations in substrate characteristics will also be conducted. In Task 2 data gathered in previous years will be prepared for publication and a simple numerical model of small crater production and destruction will be used in data interpretation.

d) Clark R. Chapman, Jayne C. Aubele, Wm. James Roberts and James A. Cutts. Sub-kilometer lunar craters: Origins, ages, processes of degradation and implications for mare basalt petrogenesis. Lunar and Planetary Sciences Conference X Extended abstracts, 1979.